HHS Public Access

Author manuscript

Sci Signal. Author manuscript; available in PMC 2017 February 15.

Published in final edited form as:

Sci Signal. ; 9(437): ra71. doi:10.1126/scisignal.aaf1047.

Facilitation of TRPV4 by TRPV1 is required for itch transmission in some sensory neuron populations

Seungil Kim[1,2,*,†], **Devin M. Barry**[1,2,*], **Xian-Yu Liu**[1,2,*], **Shijin Yin**[1,2], **Admire Munanairi**[1,2], **Qing-Tao Meng**[1,3], **Wei Cheng**[4], **Ping Mo**[1,5], **Li Wan**[1,‡], **Shen-Bin Liu**[1,2], **Kasun Ratnayake**[6], **Zhong-Qiu Zhao**[1,2], **Narasimhan Gautam**[2,7], **Jie Zheng**[8], **W. K. Ajith Karunarathne**[6], and **Zhou-Feng Chen**[1,2,9,10,§]

[1]Center for the Study of Itch, Washington University School of Medicine, St. Louis, MO 63110, USA

[2]Department of Anesthesiology, Washington University School of Medicine, St. Louis, MO 63110, USA

[3]Department of Anesthesiology, Renmin Hospital of Wuhan University, Wuhan, Hubei 430060, P.R. China

[4]Institute of Cancer Stem Cell, Dalian Medical University, Dalian 116044, P.R. China

[5]Department of Anesthesiology, Nanhai Hospital of Southern Medical University, Foshan 528000, P.R. China

[6]Department of Chemistry and Biochemistry, University of Toledo, Toledo, OH 43606, USA

[7]Department of Genetics, Washington University School of Medicine, St. Louis, MO 63110, USA

[8]Department of Physiology and Membrane Biology, University of California School of Medicine, Davis, CA 95616, USA

[9]Department of Psychiatry, Washington University School of Medicine, St. Louis, MO 63110, USA

[10]Department of Developmental Biology, Washington University School of Medicine, St. Louis, MO 63110, USA

Abstract

The transient receptor potential channels (TRPs) respond to chemical irritants and temperature. TRPV1 responds to the itch-inducing endogenous signal histamine, and TRPA1 responds to the

[§]Corresponding author. chenz@wustl.edu.
[*]These authors contributed equally to this work.
[†]Present address: Department of Cell and Tissue Biology, Program in Craniofacial Biology, University of California, San Francisco, San Francisco, CA 94143, USA.
[‡]Present address: Department of Anesthesiology, The Second Affiliated Hospital, Guangzhou Medical University, Guangzhou 510260, P.R. China.

Author contributions: S.K., D.M.B., and X.-Y.L. performed behavioral, molecular, and biochemical experiments; S.Y. and S.-B.L. performed electrophysiological recordings; W.K.A.K., A.M., K.R., and W.C. performed FRET experiments; Q.-T.M., P.M., and L.W. performed behavioral tests and data analysis; Z.-Q.Z. helped with immunohistochemistry; N.G., W.K.A.K., and J.Z. supervised FRET experiments; Z.-F.C. conceived and supervised the project; and S.K., D.M.B., X.-Y.L., and Z.-F.C. wrote the article.

Competing interests: The authors declare that they have no competing interests.

Data and materials availability: There are no restrictions on the data or materials used in this study.

itch-inducing chemical chloroquine. We showed that, in sensory neurons, TRPV4 is important for both chloroquine-and histamine-induced itch and that TRPV1 has a role in chloroquine-induced itch. Chloroquine-induced scratching was reduced in mice in which TRPV1 was knocked down or pharmacologically inhibited. Both TRPV4 and TRPV1 were present in some sensory neurons. Pharmacological blockade of either TRPV4 or TRPV1 significantly attenuated the Ca^{2+} response of sensory neurons exposed to histamine or chloroquine. Knockout of *Trpv1* impaired Ca^{2+} responses and reduced scratching behavior evoked by a TRPV4 agonist, whereas knockout of *Trpv4* did not alter TRPV1-mediated capsaicin responses. Electrophysiological analysis of human embryonic kidney (HEK) 293 cells coexpressing TRPV4 and TRPV1 revealed that the presence of both channels enhanced the activation kinetics of TRPV4 but not of TRPV1. Biochemical and biophysical studies suggested a close proximity between TRPV4 and TRPV1 in dorsal root ganglion neurons and in cultured cells. Thus, our studies identified TRPV4 as a channel that contributes to both histamine- and chloroquine-induced itch and indicated that the function of TRPV4 in itch signaling involves TRPV1-mediated facilitation. TRP facilitation through the formation of heteromeric complexes could be a prevalent mechanism by which the vast array of somatosensory information is encoded in sensory neurons.

INTRODUCTION

Transient receptor potential channels (TRPs) play important roles in transmitting a wide range of somatosensory stimuli, including itch, pain, temperature, and mechanosensation (1–4). TRPs convey itch signals in response to histamine or chloroquine (CQ). Histamine is a prototypical pruritogen that mediates allergic and inflammatory responses predominantly through the histamine H1 receptor (H1R) (5) and, to a lesser extent, H4R (6), which are G protein (heterotrimeric guanine nucleotide–binding protein)–coupled receptors (GPCRs), in dorsal root ganglion (DRG) neurons. In contrast, CQ is a prototypical pruritogen for histamine-independent (non-histaminergic) itch; systemic use in the treatment of malaria frequently causes severe pruritus (7). CQ-induced itch is mediated primarily through a pair of GPCRs, the Mas-related GPCR A3 (MRGPRA3) in sensory neurons (8) and the gastrin-releasing peptide receptor (GRPR) in the spinal cord (9). Understanding of TRP signaling mechanisms that distinguish histaminergic and nonhistaminergic itch is of therapeutic importance; most intractable chronic itch is resistant to antihistamines.

Although more than a dozen TRPs have been identified in DRG neurons (10), to date, only TRPV1, TRPA1, and TRPV4 have been implicated in itch signaling in sensory neurons (3, 11). TRPV1 functions downstream of H1R to relay histamine itch (12–14), whereas TRPA1 couples to MRGPRA3 to relay CQ-induced itch and to MRGPRC11 to relay bovine-adrenal-medulla 8–22 peptide (BAM8–22)–induced itch (8, 12, 15). TRPV4 is required for serotonin (5-hydroxytryptamine)–induced itch (11), but a role for TRPV4 in sensory neurons responding to histamine has not been reported. Although TRPV1 activity is important for H1R signaling in DRG, mice lacking *Trpv1* retain partial histamine-evoked scratching behavior (13, 14). Ca^{2+} imaging studies indicate that half of DRG neurons that respond to CQ do not respond to TRPA1 agonists, yet CQ-induced Ca^{2+} responses are blocked by the general TRP blocker ruthenium red (16), suggesting the involvement of other TRP channels for CQ-induced signaling. Moreover, genetic deletion of the *Mrgpr* gene cluster or ablation

of MRGPRA3-positive neurons partially attenuates CQ-induced itch (8, 17). Together, these studies suggest that additional TRPs may be involved in itch signaling induced by CQ or histamine.

Here, we examined the role of TRPV4 in itch and tested the hypothesis that TRPV1 and TRPV4 cooperate to relay itch information in sensory neurons. Using a combination of biochemistry, biophysics, behavior, and electrophysiology approaches, we uncovered previously unknown functions for TRPV4 and TRPV1 in itch responses induced by histamine or CQ. Our studies suggested that TRPV1 and TRPV4 form complexes to relay itch signals in a subset of DRG sensory neurons.

RESULTS

Trpv4 is expressed in sensory neurons involved in itch

We examined the expression pattern of *Trpv4* in mouse DRG neurons. In situ hybridization showed that about 24% (375 of 1565) of mouse DRG neurons expressed *Trpv4* (Fig. 1). To determine whether *Trpv4* and *Mrgpra3* expressions overlap, we performed double fluorescence in situ hybridization and found that most DRG neurons expressing *Mrgpra3* (87%, 62 of 71) were *Trpv4*-positive (Fig. 1, A and B). Histamine receptor 1 (encoded by *Hrh1*) is a key receptor that mediates histamine itch in DRG neurons (6). Double fluorescence in situ hybridization showed that 100% (78 of 78) of *Hrh1*-expressing neurons also expressed *Trpv4* (Fig. 1, C and D). *Trpv4* was also expressed in 70% (196 of 282) of *Trpv1*-expressing neurons (Fig. 1, E and F) and in 54% (91 of 169) of *Trpa1*-expressing neurons (Fig. 1, G and H). These results indicate that *Trpv4* is expressed in subsets of sensory neurons that may be involved in CQ- or histamine-induced itch or in neurons that may respond to both pruritogens.

TRPV4 is required for both CQ- and histamine-induced itch

To determine whether TRPV4 is required for itch transmission, we examined scratching behaviors of mice lacking *Trpv4* (18) after intradermal injection of histamine or CQ. Compared with wild-type littermates, *Trpv4*$^{-/-}$ mice exhibited a significant attenuation in scratching responses to both CQ and histamine (Fig. 2A). We next performed pharmacological blockade of TRPV4 using intraperitoneal injection of HC 067047 (HC), a specific TRPV4 antagonist (19). Consistently, HC markedly reduced scratching bouts evoked by histamine or CQ relative to the vehicle control (Fig. 2B).

In addition to DRGs, TRPV4 is present in skin keratinocytes (20). To ascertain whether TRPV4 is intrinsically required in DRG neurons for CQ and histamine itch, we performed small interfering RNA (siRNA) knockdown of *Trpv4* in DRG neurons by intrathecal injection of the siRNA. We observed a significant reduction of scratching responses elicited by either CQ or histamine in mice injected with the *Trpv4* siRNA, when compared to mice injected with negative control siRNA (Fig. 2C). Moreover, scratching bouts induced by intradermal injection of GSK1016790A (GSK101), a specific small-molecule agonist for TRPV4 both in vivo and in vitro (21, 22), were significantly attenuated in mice receiving the *Trpv4* siRNA compared with those injected with control siRNA (Fig. 2C). qRT-PCR

analysis confirmed the knockdown of *Trpv4* mRNA in DRGs relative to the Trpv4 transcript abundance in DRGs from mice receiving the control siRNA and confirmed that *Trpv1*, *Trpv2*, *Trpa1*, and *Trpm8* were unaffected (Fig. 2D). Western blot analysis confirmed that the abundance of TRPV4 protein in DRGs was also significantly reduced in *Trpv4* siRNA–treated mice relative to that in the siRNA control mice (Fig. 2E).

The presence of both TRPV4 in neurons with TRPV1 or TRPA1 raised the possibility that TRPV4 could function in concert with TRPV1 or TRPA1 in itch signaling. To test this, we compared the scratching response induced by intradermal injection of GSK101 in *Trpv4*$^{-/-}$ (18), *Trpa1*$^{-/-}$ (23), and *Trpv1*$^{-/-}$ (24) mice with the response of their wild-type littermates. GSK101-induced scratching behavior was significantly attenuated in *Trpv4*$^{-/-}$ and *Trpv1*$^{-/-}$ mice, but not in *Trpa1*$^{-/-}$ mice (Fig. 2F), indicating that TRPV4-mediated scratching response is independent of TRPA1 and that TRPV1 is involved in TRPV4-mediated itch.

TRPV1 is required for CQ-induced itch in a TRPV4-dependent manner

The finding that the response to TRPV4 required TRPV1 prompted us to revisit the role of TRPV1 in CQ itch. Consistent with previous report (13), *Trpv1*$^{-/-}$ mice showed impaired scratching response to histamine but not to CQ (Fig. 3A). However, *Trpv1* knockout may result in compensatory changes in DRG neurons (25). To avoid the potential compensatory effect that may underlie the normal CQ itch in *Trpv1*$^{-/-}$ mice, we blocked TRPV1 activity by intraperitoneal injection of SB 366791 (SB), a specific TRPV1 antagonist in vitro and in vivo (26, 27). SB attenuated not only histamine-induced itch but also CQ-induced itch (Fig. 3B). Knocking down *Trpv1* in adult mice by intrathecal injection of siRNA against *Trpv1* also diminished the scratching response induced by histamine or CQ (Fig. 3C). We confirmed the specificity of the *Trpv1* siRNA by qRT-PCR (Fig. 3D) and that TRPV1 abundance was significantly reduced in DRGs of *Trpv1* siRNA–injected mice (Fig. 3E). These results indicated that TRPV1 is involved in CQ- and histamine-induced itch.

Our findings raised an important question about whether TRPV1 and TRPV4 work in concert or independently to relay CQ itch. Therefore, we evaluated the relationship between TRPV4 and TRPV1 in histamine- and CQ-induced itch using siRNA knockdown in the *Trpv4*$^{-/-}$ background. *Trpv1* siRNA knockdown in *Trpv4*$^{-/-}$ mice almost abolished scratching behavior evoked by histamine when compared to control siRNA–injected *Trpv4*$^{-/-}$ mice (Fig. 3F). Mice lacking both TRPV4 and TRPV1 functions that were not exposed to itch-inducing molecules scratch a similar amount as these mice when exposed to histamine (scratches in 30 min in the absence of histamine 11 ± 6, $n = 7$ mice; scratches induced by histamine 8 ± 3, $n = 6$ mice). By contrast, *Trpv1* siRNA knockdown did not further attenuate CQ-induced itch in *Trpv4*$^{-/-}$ mice (Fig. 3G). These results suggested that the function of TRPV1 in CQ-induced itch depended on the presence of TRPV4, whereas in histamine-induced itch TRPV1 may have both TRPV4-dependent and TRPV4-independent activities.

TRPV1 increases the proportion of sensory neurons that respond to a TRPV4 agonist

The observation that GSK101-induced scratching behavior was significantly reduced in *Trpv1*$^{-/-}$ mice compared to that in wild-type littermates (Fig. 2F) raised the question of whether or not GSK101 is a partial agonist for TRPV1. Therefore, we examined GSK101-induced Ca^{2+} responses in dissociated DRG neurons using calcium imaging. Consistent with previous studies (21), we did not detect GSK101-responsive neurons in *Trpv4*$^{-/-}$mice, whereas in wild-type mice about 13% of the neurons that could be activated by depolarization with KCl responded to GSK101 (Fig. 4, A and B). Capsaicin is a specific agonist of TRPV1 (24, 28), and the percentage of capsaicin-responsive neurons was similar in the DRGs from *Trpv4*$^{-/-}$and wild-type mice (42% in wild-type mice and 38% in the *Trpv4*$^{-/-}$; Fig. 4B), indicating that the function of TRPV1 does not require TRPV4. We also tested GSK101 at a concentration greater than 1 μM. Whereas the percent of GSK101-responsive neurons increased in a dose-dependent manner to 1 μM GSK101, the percent of responsive neurons was similar between 1 and 10 μM (Fig. 4C). Because the proportion of GSK101-responsive neurons was significantly less than that of capsaicin-responsive neurons even at the highest concentration of GSK101 tested (10 μM), we concluded that GSK101 is specific for TRPV4 and did not activate TRPV1. In contrast, in the DRG neurons from *Trpv1*$^{-/-}$ mice, capsaicin did not evoke a Ca^{2+} response, and the proportion of GSK101-responsive neurons was significantly reduced compared to that of DRGs from wild-type mice (Fig. 4, D and E). These data suggested that TRPV1 enhanced the responsiveness of a subset of DRG neurons to TRPV4 stimulation but that TRPV1 activation by capsaicin was independent of TRPV4.

Antagonizing either TRPV4 or TRPV1 reduces CQ- and histamine-induced Ca^{2+} signaling

To determine whether antagonism of TRPV4 or TRPV1 attenuated Ca^{2+} responses evoked by GSK101, CQ, or histamine in sensory neurons in the DRG, we used a two-step paired protocol and compared the differences in the amplitude of intracellular Ca^{2+} concentration ($[Ca^{2+}]_i$) with or without antagonist. The advantage of this paired protocol is that we can identify the pruritogen-responsive neurons in the first step and then determine the effect of the antagonist in the second step. Through this procedure, we can exclude neurons that are not involved in mediating itch responses.

We identified TRPV4-positive neurons with GSK101, washed out the agonist, applied an antagonist or a control (vehicle), and then added GSK101 without washing out the antagonist or vehicle (Fig. 4F). We compared the amplitudes of $[Ca^{2+}]_i$ of the first response and the second response. Application of the TRPV4 antagonist HC blocked GSK101-induced responses (~92% decrease), and the TRPV1 antagonist SB reduced GSK101-induced responses (~38% decrease) (Fig. 4G). The response of the TRPV4-positive neurons to CQ (Fig. 4, H and I) or histamine (Fig. 4, J and K) was also significantly reduced by either HC or SB. Collectively, these data indicated that TRPV1 contributed to the response to CQ and histamine in TRPV4-positive sensory neurons.

To determine the proportion of DRG neurons that responded to CQ, histamine, or capsaicin, and also to GSK101, we used *Pirt-GCaMP3* mice, which express a fluorescent Ca^{2+} indicator specifically in sensory neurons (28). We detected GSK101-evoked Ca^{2+} responses

in neurons that also responded to CQ, histamine, or capsaicin (Fig. 5, A and B). Of the 1493 neurons examined, 170 were activated by GSK101, and of the GSK101-responsive neurons, ~50% were also responsive to both CQ and histamine (Fig. 5C). Furthermore, similar proportions of GSK101-responsive neurons responded to CQ [52% (89 of 170)] as CQ-responsive neurons responded to GSK101 [58% (89 of 154)]. Similar proportions also existed between GSK101- and histamine-responsive neurons: 57% (97 of 170) of GSK101-responsive neurons were histamine-responsive, and 62% (97 of 156) of histamine-responsive neurons also responded to GSK101 (Fig. 5C). Most of the GSK101-responsive neurons (79%, 135 of 170), CQ-responsive neurons (83%, 128 of 154), and histamine-responsive neurons (81%, 132 of 163), as defined by the first step in the two-step paired protocol, also responded to capsaicin (Fig. 5, D and E), which is consistent with previous studies (12, 29) and indicates that TRPV1 is broadly distributed in itch-sensing neurons. Furthermore, the data indicated that TRPV4 and TRPV1 activities are present in most sensory neurons that respond to both CQ and histamine.

TRPV1 facilitates TRPV4-mediated itch responses

To examine whether TRPV1 and TRPV4 had additive effects on itch transmission, we tested the effect of intraperitoneal injection of both TRPV1 and TRPV4 antagonists (SB and HC, respectively) on itch behavior at doses that were insufficient to individually block CQ-induced itch (Fig. 6A). However, co-injection of HC and SB significantly reduced CQ-induced scratching (Fig. 6A). These results indicated that the antagonists were not producing an additive effect. To test for facilitation of TRPV4-dependent responses by TRPV1, we used the two-step paired protocol and monitored Ca^{2+} responses in sensory neurons. Neurons positive for both TRPV4 and TRPV1 were identified by sequential application of GSK101 and then capsaicin (Fig. 6B), the lowest concentrations that evoked Ca^{2+} responses. Coapplication of GSK101 and capsaicin resulted in a significantly greater response than the response evoked by either agonist alone (Fig. 6, B and C, purple trace). As a control, we showed that neurons responding only to capsaicin and not GSK101 did not produce an increased response when both capsaicin and GSK101 were applied (Fig. 6, B and D, blue trace). Together, these data suggested that TRPV1 facilitates TRPV4-mediated itch signaling in sensory neurons.

TRPV4 and TRPV1 form complexes in DRG neurons and are in close proximity when expressed in HEK293 cells

The scratching behavior and Ca^{2+} imaging analysis suggested that TRPV4 and TRPV1 may function as part of a complex. TRPV1 and TRPV4 coimmunoprecipitated from DRG membrane preparations (Fig. 7A, left panel for TRPV4, middle panel for TRPV1, lane 4). In contrast, these proteins were not detectable either when an irrelevant antibody was used (Fig. 7A, lane 2) or in the absence of the DRG membranes (Fig. 7A, lane 3). The absence of TRPV4 in *Trpv4*$^{-/-}$ DRG membranes confirmed the specificity of the TRPV4 antibody (Fig. 7A, right panel). These results indicated that TRPV4 and TRPV1 form a complex in DRG neurons.

We performed fluorescence resonance energy transfer (FRET) experiments using cyan fluorescent protein (CFP) and enhanced yellow fluorescent protein (eYFP) as paired

fluorophores in human embryonic kidney (HEK) 293 cells cotransfected with TRPV4-CFP and TRPV1-eYFP, TRPV4-eYFP, or TRPA1-eYFP. Because FRET requires the donor (CFP) to be in close proximity (1 to 10 nm) to the acceptor (eYFP), positive FRET signals observed from the plasma membranes indicate close proximity of the tagged TRPV channels (30, 31). FRET efficiency was calculated as the eYFP emission due to energy transfer, by fitting the FRET model to each coexpression experiment (31). We observed FRET efficiency of 18%, 11%, and 9% in cells cotransfected with TRPV4-CFP/TRPV4-eYFP, TRPV4-CFP/TRPV1-eYFP, and TRPV4-CFP/TRPA1-eYFP, respectively (Table 1). To avoid variations due to cell-to-cell heterogeneity, we performed spatially confined photobleaching of the acceptor (eYFP) (Fig. 7B, yellow box). After acceptor photobleaching of TRPV1-eYFP, fluorescence intensity of TRPV4-CFP (donor) increased due to the loss of energy transfer (Fig. 7C, blue trace), suggesting that the two channels were in close enough proximity for FRET to occur. The nonphotobleached region of the same cell served as an internal control (Fig. 7D). Both FRET analysis and the change in signal after photobleaching indicated that TRPV4 homomultimerized (Table 1 and Fig. 7E). In contrast, cells coexpressing TRPV4-CFP and TRPA1-eYFP did not show an increase in the acceptor signal after photo-bleaching (Fig. 7F). These data indicated that TRPV4 can form homomeric and heteromeric complexes with TRPV1.

TRPV1 enhances the rate of activation of TRPV4 when coexpressed in HEK293 cells

To investigate the functional effects of this interaction between TRPV1 and TRPV4 in a controlled system, we expressed TRPV4 with or without TRPV1 and TRPA1 in HEK293 cells and performed electrophysiological analysis. HEK293 cells expressing only TRPV1 are not activated by GSK101 (32). We recorded GSK101-activated whole-cell membrane currents using voltage ramps from −100 to +100 mV and defined the time course of onset and recovery from GSK101-induced activation to calculate activation efficacy. GSK101 activated a large and almost linear current in TRPV4-expressing cells, TRPV4- and TRPV1-coexpressing cells, or TRPV4- and TRPA1-coexpressing cells (Fig. 8, A to C). Although the current densities activated by GSK101 were similar (Fig. 8D), indicating a similar abundance of the channels at the plasma membrane, the time course of onset and recovery from GSK101 activation displayed differences among these cells (Fig. 8E). At −60 mV, the estimated dissociation constant (K_d) for activation by GSK101 in TRPV4- and TRPV1-coexpressing cells was 16.4 ± 5.2 nM, which was significantly lower than the K_d in cells expressing TRPV4 alone (48.6 ± 8.0 nM) or in cells coexpressing TRPV4 and TRPA1 (28.6 ± 7.7 nM) (Fig. 8F). Although the activation K_d was less in the cells coexpressing TRPV4 and TRPA1 than in those expressing only TRPV4, the difference was not significant. These findings showed that the presence of TRPV1 facilitates TRPV4 activation in HEK293 cells.

To determine whether TRPV4 reciprocally enhanced TRPV1-mediated activity, we analyzed capsaicin-activated whole-cell membrane currents in HEK293 cells. Capsaicin activated a large and almost linear current in TRPV1-expressing cells or in TRPV4- and TRPV1-coexpressing cells (Fig. 8, G and H). Current densities for capsaicin-induced responses were similar in these cells (Fig. 8I). The time course of onset and recovery from capsaicin-stimulated activation were also similar (Fig. 8J), yielding nearly identical activation K_d: Cells expressing TRPV1 had an activation K_d of 70.9 ± 24.2 nM, and those expressing both

TRPV4 and TRPV1 had an activation K_d of 71.5 ± 17 nM (Fig. 8K). Thus, TRPV4 does not modulate TRPV1 activation when the two channels are coexpressed in HEK293 cells.

DISCUSSION

Using a multidisciplinary approach combining genetics, biochemistry, and biophysics, as well as electrophysiological and behavioral studies, we examined the relationship between TRPV1 and TRPV4 in transmission of itch signals. We showed that both TRPV1 and TRPV4 contributed to CQ- and histamine-induced scratching behavior. Our data also indicated that TRPV1 and TRPV4 function in complexes both in neurons of the DRG and when expressed in HEK293 cells. Furthermore, pharmacological, behavioral, Ca^{2+} imaging, and electrophysiological studies indicated that the function of TRPV4 in itch signaling depended on TRPV1 and that TRPV1 facilitates the responsiveness of TRPV4 to pruritogenic stimuli.

Our finding that TRPV1 was required for CQ-induced itch is surprising, because previous studies of *Trpv1*$^{-/-}$ mice indicated that this TRP channel was not involved (12, 15). This discrepancy can be explained by the distinct approaches used and the possibility of adaptation in the knockout mice. Some aspects of TRPV1 function are compensated in *Trpv1*$^{-/-}$ mice (25). For example, *Trpv1*$^{-/-}$ mice exhibit normal mechanical pain hypersensitivity (24, 33), but studies using molecular and pharmacological blockade in adult mice indicate that TRPV1 is important for this response (34). Because we used TRPV1 antagonist SB and knockdown to show the involvement of TRPV1 in CQ-induced itch, our experimental approaches should avoid developmental or functional compensation that may occur in the *Trpv1*$^{-/-}$ mice. Compensation is most likely stimulus- and state-dependent—manifesting in one phenotype but not others—depending on the involvement of various TRPs. Although TRPV1 is also present in spinal γ-aminobutyric acid–releasing interneurons (35), where it functions in nociceptive processing, we think unlikely that spinal TRPV1 accounts for the scratching behavior that we observed. The present findings are consistent with previous studies implying a role for TRPV1 in CQ itch: Coapplication of the TRPV1 agonist capsaicin and QX-314, a sodium channel blocker that is permeable through open TRP channel pores, significantly attenuated CQ-evoked scratching behavior (12). In addition, CQ not only excites 25% of TRPV1-positive neurons but also sensitizes TRPV1 to capsaicin in about 52% of TRPV1-positive neurons (16). Thus, we conclude that TRPV1 contributes to CQ-induced signaling and scratching behaviors.

We also showed that TRPV4 is a key channel in sensory neurons and contributes to itch perception of both CQ and histamine. Although we found that *Trpv1* and *Trpv4* are expressed in overlapping sets of DRG neurons, *Trpv1* siRNA knockdown in *Trpv4*$^{-/-}$ mice failed to further reduce the residual CQ-induced scratching behavior, suggesting that the requirement of TRPV1 for CQ-induced itch involves the population of neurons that have both TRPV1 and TRPV4. In contrast, knocking down TRPV1 in *Trpv4*$^{-/-}$ mice further reduced histamine-induced scratching, indicating that TRPV1 conveys histamine-induced itch through neurons that have both TRPV1 and TRPV4 and those that have TRPV1 but lack TRPV4 (Fig. 9A). Whereas the pattern of *Trpa1* expression overlapped with that of *Trpv4* and *Trpv1*, our studies suggested that TRPA1 transmits CQ-induced itch in a TRPV4- and

TRPV1-independent manner (Fig. 9, B and C). Further experiments are required to clarify the relation between TRPA1 and TRPV4 or TRPV1.

MRGPRA3 relays CQ-induced itch by stimulating TRPA1 in ~5 to 7% of sensory neurons (8, 15). The observation that deletion of the *Mrgpr* gene cluster or ablation of *Mrgpra3*-expressing DRG neurons only partially attenuates CQ-induced itch (8, 17) is consistent with our finding that additional subsets of DRGs, including those that are positive for both TRPV4 and TRPV1, are involved in CQ-induced itch. Which GPCR relays this signal to TRPV4 and TRPV1 remains to be determined, as well as which GPCR relays histamine-induced itch in these neurons. Nevertheless, our studies showed that TRPV4-positive neurons that respond to both CQ and histamine comprise two subpopulations—those that only have TRPV4 and those that have both TRPV4 and TRPV1 (Fig. 9D). The current study does not exclude the possibility that additional TRPs are involved in CQ- and histamine-induced itch but does define several distinct TRP pathways for relaying CQ and histamine itch (Fig. 9, D and E).

Another study by Akiyama *et al.* showed that TRPV4 is not required for histamine-induced itch and, more markedly, that CQ-induced itch is increased in *Trpv4*$^{-/-}$ mice (11). Exon 12, which encodes the pore loop and adjacent transmembrane domain, is deleted in the *Trpv4*$^{-/-}$ mice that Akiyama *et al.* used (36). It is possible that this may result in a truncated TRPV4 protein with altered activity. Although the mutant mouse was verified by immunostaining with kidney protein extracts, the TRPV4 antibody used recognized the C-terminal peptide sequence, which may not detect a truncated protein (36). In contrast, in the *Trpv4*$^{-/-}$ mice that we used, exon 4, which encodes the ankyrin repeat domain, was replaced (18), and the absence of TRPV4 transcript and protein was shown by RT-PCR and immunohistochemistry in DRG sensory neurons (18). Moreover, the ankyrin repeat domain is conserved in TRPV1, TRPV3, and TRPV4 and is important for protein-protein interactions and also harbors the site of ATP (adenosine 5′-triphosphate) and calmodulin binding, which is critical for TRP channel sensitivity for activation (37). This is particularly relevant to the present findings, because deletion of the ankyrin repeat domain may compromise the formation of complexes between TRPV1 and TRPV4. Moreover, mutations in this domain cause human congenital disorders by reducing membrane surface localization of functional TRPV4 channels (38). Distinct phenotypes resulting from different deletions in the same genes are not uncommon. This is especially true for large proteins, such as GPCR or TRPs, because alternative splicing events often occur if the deletion is made in the last coding exons, resulting in truncated protein with altered or partial function, which can produce gain-of-function phenotypes or unexpected phenotypes. Because of this possibility, we also used *Trpv4* knockdown approaches and confirmed reduced function by Ca^{2+} imaging of DRG neurons. The consistent deficits in histamine- and CQ-induced itch after *Trpv4* knockdown indicate that the *Trpv4*$^{-/-}$ mice that we used represent a functional null mutation.

Our behavioral and Ca^{2+} imaging studies showed that TRPV1 deficiency or antagonism impairs TRPV4 responses. Conversely, the presence of TRPV1 even without adding a TRPV1-specific agonist altered the response and activation kinetics of TRPV4 to GSK101. In contrast, TRPV4 deficiency did not influence the response of TRPV1, and its presence did not affect the response of TRPV1 to capsaicin. Because GSK101 did not activate

TRPV1, these observations indicated a pivotal role for TRPV1 in facilitation of TRPV4 function. Furthermore, coapplication of a low dose of both a TRPV1 and a TRPV4 antagonist—each at half the amount of an insufficient dose—attenuated scratching evoked by CQ, indicating that their effects were not independent and additive. This conclusion is supported by the observation that coapplication of agonists at low concentrations evoked Ca^{2+} responses that were greater in magnitude than Ca^{2+} responses evoked by agonists individually even at twice the concentration.

Facilitation between TRPV4 and TRPV1 in sensory neurons occurs in various conditions. For instance, TRPV4 and TRPV1 are both activated and potentiated by stimuli that activate the GPCR PAR2, a member of the protease activated receptor family, and this has been implicated in pain signaling (39–41). Another study found that TRPV4 has a permissive role for TRPV1 function in central thermosensory neurons (42). Thus, the close proximity that we detected between TRPV1 and TRPV4 may provide a mechanism for their regulation by the signaling effectors, such as phosphatidylinositol 4,5-phosphate, downstream of the GPCRs activated by pruritogens. Intracellular signaling molecules, such as ATP and calmodulin, may bind to the conserved regions in TRP channels at spatially discrete microdomains of the cell so that activation of one channel modulates the activity of the other and insulates them from the interfering effect of other TRPs (37, 43). Although our studies indicated that TRPV1 and TRPV4 may form a functional complex, our results do not exclude the possibility that TRPV1 can also facilitate TRPV4 activity without forming a complex. Whether facilitation occurs at the plasma membrane or involves enhanced trafficking to the cell surface or directs the channels to specific regions of the cell (44) remains to be determined.

TRPV4 has emerged as a versatile channel that coassembles with other types of TRPs (31, 44–46). Functional synergism between TRPV1 and TRPV4 was first reported in *Caenorhabditis elegans*, suggesting that cross-facilitation of TRPs may be evolutionarily conserved (47). Given the overlapping expression of TRP-encoding genes and the “lack of” phenotype for anticipated function in mice lacking a single TRP, TRP cross-facilitation may be a common mechanism for cellular “computation” that produces specific behaviors or mediates specific sensory modalities. Dynamic cross-facilitation of distinct TRPs in response to physiological and pathological stimuli would expand the functionality of TRPs as versatile sensors for encoding and transmitting a vast array of environmental stimuli.

MATERIALS AND METHODS

Double fluorescence in situ hybridization and immunohistochemistry

For double fluorescence in situ hybridization, complementary RNA probes for *Trpv4*, *Mrgpra3*, and *Hrh1* were labeled with fluorescein and digoxigenin (Roche). Fluorescein-labeled probe was purified through a G50 microcolumn (Amersham Pharmacia) and then precipitated with lithium chloride ($LiCl_2$). Two probes were added into a hybridization buffer. Probes were detected with an antibody recognizing fluorescein (1:2000, Roche) or an antibody recognizing digoxigenin (1:2000, Roche). Antibody staining after in situ hybridization to detect *Trpv4* was performed as described (8, 48). Slides were examined using an Olympus BX51 upright microscope attached with a CCD (charge-coupled device)

camera. The following primary and secondary antibodies were used: rabbit antibody recognizing TRPV1 (1:1000, Neuromics, cat. no. RA14113), rabbit antibody recognizing TRPA1 (1:50, Ardem Patapoutian Lab), and fluorescein isothiocyanate–coupled donkey antibody recognizing rabbit IgG (1:400, Jackson ImmunoResearch). The TRPV1 antibody was previously validated using wild-type and *Trpv1*$^{-/-}$ tissues (49). The TRPA1 antibody was previously validated using wild-type and *Trpa1*$^{-/-}$ tissues (50).

Mice

Adult male C57BL/6J mice, *Trpv4*$^{-/-}$ mice (18), *Trpv1*$^{-/-}$ mice, *Trpa1*$^{-/-}$mice, wild-type littermates, and *Pirt-GCaMP3* mice (28) were used for the study (all strains were in C57BL/6J background). Mice were housed in clear plastic cages with no more than five mice per cage in a controlled environment at a constant temperature of 23°C and humidity of 50 ± 10% with food and water available ad libitum. The animal room was on a 12:12-hour light-dark cycle with lights on at 7 a.m. Male mice 7 to 12 weeks old were used for experiments. Age-matched animals, tissues, and cells for culture were used or collected randomly for each group in each experiment. The animal experiments were performed in accordance with the guidelines of the National Institutes of Health and were approved by the Animal Studies Committee at Washington University School of Medicine. C57BL/6J and *Trpv1*$^{-/-}$ mice (24) were purchased from the Jackson Laboratory. *Trpa1*$^{-/-}$ mice (23) were from G. Story. *Trpv4*$^{+/-}$ mice (18) (RIKEN BioResource Center, Japan) were bred to generate *Trpv4*$^{-/-}$ mice.

Acute scratching behavior

Scratching behaviors were performed as previously described (51, 52). All behavior was performed during the light cycle. Briefly, the injection area was shaved 2 days before experiments. Before the experiments, each mouse was placed in a plastic arena (10 cm × 11 cm × 15 cm) for 30 min to acclimate. Mice were briefly removed from the chamber and intradermally injected at the back of the neck with CQ (200 μg in 50 μl of saline; Sigma), histamine (200 μg in 50 μl of saline; Sigma), or GSK101 [10 μg in 50 μl of saline containing 2% dimethyl sulfoxide (DMSO); Sigma]. For antagonist experiments, the TRPV4 antagonist HC (Tocris Bioscience) and the TRPV1 antagonist SB (Tocris Bioscience) were first dissolved in 100% DMSO and diluted with saline. Animal behaviors were videotaped (Sony, HDR-CX190) from a side angle and played back on a computer for assessments by observers blinded to the treatments and the genotypes of the animals. Hindlimb scratching behavior toward the injected area was observed for 30 min with 5-min intervals. One bout of scratch was defined as a lifting of the hindlimb to the injection site and then a replacing of the limb back to the floor or to the mouth, regardless of how many scratching strokes take place in between (9).

siRNA treatment

MISSION siRNA Universal Negative Control #1 (SIC001) and selective siRNA duplex for mouse *Trpv4* mRNA (SASI_Mm01_00182300) and *Trpv1* mRNA (SASI_Mm01_00041084) were purchased from Sigma. RNA was dissolved in diethyl pyrocarbonate–treated PBS and prepared immediately before administration by mixing the RNA solution with a transfection reagent, in vivo-jetPEI (Polyplus-transfection SA). The

final concentration of RNA was 1.25 μg/10 μl. siRNA was delivered to the lumbar region of the spinal cord. Injection was given twice daily for six consecutive days. Behavioral tests for CQ, histamine, and GSK101 were carried out 24 hours after the last injection with 3 hours of rest in between tests. Lumbar DRGs were then dissected out from control and siRNA-treated mice and stored in RNAlater at −80°C or rapidly frozen in dry ice until RT-PCR or Western blot analysis.

Quantitative reverse transcription polymerase chain reaction

Lumbar DRGs were homogenized with a Dounce glass homogenizer, and total RNA was prepared by using TRIzol reagent (Invitrogen). Complementary DNA (cDNA) was synthesized using SuperScript First-Strand Synthesis System (Invitrogen), and conventional or qRT-PCR was performed using iQ SYBR Green Supermix (Bio-Rad) and Mx3000P QPCR System (Stratagene). Expression of target mRNA was normalized to 18*S* ribosomal RNA abundance. The following primers are used for PCR: 18*S* RNA, 5′-AAACGGCTACCACATCCAAG-3′ and 5′-CCTCCAATG-GATCCTCGTTA-3′; *Trpv1*, 5′-GTGATCGCCTACAGTAGCAGTG-3′ and 5′-ACATGTGGAATACAGGCTGTTG-3′; *Trpv2*, 5′-GGTGGTTTTAGAGCCACTGAAC-3′ and 5′-GTAGATGCCTG-TGTGCTGAAAG-3′; *Trpv4*, 5′-GAGAACACCAAGTTTGTCACCA-3′ and 5′-TGAATCATGATGCTGTAGGTCC-3′; *Trpa1*, 5′-AGTATCAT-CTTCGTGTTGCCCT-3′ and 5′-AGTCTCCCACTCCCATAAGACA-3′; *Trpm8*, 5′-ATGAATATGAGACCCGAGCAGT-3′ and 5′-GCAA-AGAGGAACAGGAAGAAGA-3′.

Western blot and densitometric analyses

Lumbar DRGs (L1 to L6) dissected from siRNA-treated mice and control mice were homogenized with sonication in 200 μl of ice-cold RIPA (radioimmunoprecipitation assay) buffer (50 mM Tris-HCl, pH 7.4, 150 mM NaCl, 5 mM EDTA, 1% Nonidet P-40, 0.5% sodium deoxycholate, 0.1% SDS) containing proteinase inhibitors (Sigma) as described (53). Homogenates were centrifuged at 700*g* for 10 min at 4°C. The supernatants were centrifuged at 12,000*g* for 30 min at 4°C to obtain the membrane pellets. The membrane proteins were solubilized in 20 μl of RIPA buffer containing proteinase inhibitors for subsequent SDS–polyacrylamide gel electrophoresis separation as described previously (53). Transferred blots were blocked in blocking buffer (5% nonfat dry milk in PBS and 0.1% Tween 20) for 1 hour at room temperature and incubated with rabbit antibody recognizing actin (1:5000, Sigma, cat. no. A2066) for 16 hours at 4°C. This was followed by 1-hour incubation in donkey horseradish peroxidase–linked secondary antibodies (Santa Cruz Biotechnology) at 1:5000. Immunoblots were developed with the enhanced chemiluminescence reagents (Thermo Scientific). Same blots were washed with PBS and 0.1% Tween 20 and reprobed with rabbit antibody recognizing TRPV4 (1:2000, Abcam, cat. no. ab39260) or TRPV1 (1:3000, same as described for immunohistochemistry). X-ray films were scanned, and the intensities of corresponding bands (42 kD for actin, 98 kD for TRPV4, and 95 kD for TRPV1) were measured using Kodak 1D (version 3.1.2). Optical density ratios of TRPV4/actin and TRPV1/actin were calculated to adjust loading errors.

DRG culture and Ca^{2+} imaging

DRGs were dissected in neurobasal media (Invitrogen) and incubated with papain (30 μl/2 ml neurobasal; Worthington) for 20 min at 37°C. After washing with PBS (pH 7.4), cells were incubated with collagenase (3 mg/2 ml neurobasal; Worthington) for 20 min at 37°C. After washing with PBS, cells were dissociated with a flame-polished glass pipette in neurobasal media. Dissociated cells were collected through a cell strainer (BD Biosciences) to remove tissue debris. Dissociated DRG cells were resuspended with DRG culture media (2% fetal bovine serum, 2% horse serum, 2% B-27 supplement, and 1× glutamine in neurobasal media; Invitrogen) and plated onto polyornithine–coated 12-mm-diameter round glass cover-slips in a 24-well plate. After 24 hours, cell culture media were replaced with Ca^{2+} imaging buffer (140 mM NaCl, 4 mM KCl, 2 mM $CaCl_2$, 1 mM $MgCl_2$, 5 mM glucose, 10 mM Hepes, adjusted to pH 7.4 with NaOH). Fura-2 acetoxymethyl ester (fura-2 AM) (Invitrogen) was diluted to 2 mM stock in DMSO/20% pluronic acid. Cells were loaded with fura-2 AM (2 μM) diluted in the Ca^{2+} imaging buffer. *Pirt-GCaMP3*–cultured DRG neurons were not loaded with fura-2 AM, because they express a cytoplasmic fluorescent Ca^{2+} sensor (28). The coverslips were mounted on a Warner Instruments recording chamber (RC 26G) perfused with Ca^{2+} imaging buffer at a rate of ~2 ml/min. An inverted microscope (Nikon Eclipse Ti 20× objective) with Roper CoolSNAP HQ2 digital camera was used for fura-2 Ca^{2+} imaging after 340/380-nm laser excitations (sampling interval, 2 s; exposure time adjusted for each experiment to ~70 ms for 340 nm and to ~40 ms for 380 nm). Calibration was performed to convert F_{340}/F_{380} signal ratios to $[Ca^{2+}]_i$ using Fura-2 Calcium Imaging Calibration Kit (Invitrogen) following the manufacturer's instruction. *Pirt-GCaMP3*–cultured DRG neuron fluorescence was monitored using 488-nm laser excitation of *Pirt-GCaMP3* and a 505- to 555-nm variable secondary dichroic mirror to detect the emission of green fluorescence (sampling interval, 1.5 s; exposure time adjusted for each experiment to ~200 ms). The Ca^{2+} amplitude was expressed as a normalized value of the ratio of fluorescent difference ($F_t - F_0$ or ΔF) to basal fluorescence (F_0). GSK101 (1 nM, 10 nM, 100 nM, 1 μM, or 10 μM, Sigma), CQ (1 mM, Sigma), histamine (50 μM, Sigma), capsaicin (10 or 100 nM, Sigma), KCl (30 mM, Sigma), the TRPV4 antagonist HC (10 μM, Tocris Bioscience), the TRPV1 antagonist SB (10 μM, Tocris Bioscience), or vehicle control [0.1% (v/v) DMSO] in Ca^{2+} imaging buffer) was applied to DRG cultures to examine Ca^{2+} responses. The percentage of responsive neurons was calculated from total KCl^+ neurons. NIS-Elements (version 3.1, Nikon) and Prism 6 (version 6.0e, GraphPad) were used to analyze Ca^{2+} imaging data.

Coimmunoprecipitation

DRGs were dissected on ice and quickly frozen at −80°C. For coimmunoprecipitation analysis, DRGs from five mice were pooled together, and membrane proteins were extracted as described (53). Samples were transferred into a microtube containing ice-cold sample buffer [20 mM tris-HCl (pH 7.4), 1 mM dithiothreitol, 10 mM NaF, 2 mM Na_3VO_4, 1 mM EDTA, 1 mM EGTA, 5 mM microcystin-LR, and 0.5 mM phenylmethylsulfonyl fluoride] and homogenized by sonication. Homogenates were centrifuged at 700*g* for 10 min at 4°C. The supernatant was centrifuged at 40,000*g* for 30 min at 4°C to obtain the membrane pellet. The membrane was solubilized in a sample buffer containing 0.5% sodium deoxycholate. After incubation for 20 min at 4°C, Triton X-100 was added to a final concentration of 0.5%.

Insoluble proteins were sedimented at 50,000*g* for 30 min at 4°C. The supernatants were used for coimmunoprecipitation. Two hundred micrograms of solubilized samples was incubated with a rabbit antibody recognizing TRPV4 (1 μg, Alomone Labs, cat. no. ACC-034) overnight at 4°C. The complex was precipitated with 50% TrueBlot rabbit IgG bead slurry (eBioscience). The beads were washed four times in PBS with 0.3% Triton X-100 and boiled in LDS sample buffer (Invitrogen) with 50 mM dithiothreitol for 10 min. Membrane proteins or immunoprecipitates were separated on SDS NuPAGE Bis-Tris 4 to 12% gels (Invitrogen) and transferred to polyvinylidene fluoride membrane (Invitrogen). The blots were blocked in blocking buffer (5% nonfat dry milk in PBS and 0.1% Tween 20) for 1 hour at room temperature and incubated with rabbit antibody recognizing TRPV4 (1:5000, same as described for coimmunoprecipitation) or TRPV1 (1:10,000, same as described in immunohistochemistry) for 16 hours at 4°C. This was followed by 1-hour incubation in goat horseradish peroxidase–linked TrueBlot secondary antibodies (eBioscience) at 1:5000. Immunoblots were developed with the enhanced chemiluminescence reagents (Amersham). The TRPV4 antibody was previously validated in wild-type and *Trpv4*$^{-/-}$ tissues (54).

Confocal subcellular FRET imaging

FRET signals were determined as previously described (55, 56). The fluorophores used in the present study are cerulean (which is a brighter version of the CFP) and the eYFP. Plasmids encoding the TRP channel subunit fused with either cerulean or eYFP at its C terminus were generated and cotransfected into HEK293 cells. Fluorescence imaging was done at 37°C, 24 hours after transfection. Right before fluorescence recording, the culture media were replaced with Hank's balanced salt solution supplemented with glucose (1 mg/ml). Confocal imaging and instantaneous acceptor photobleaching experiments were performed using an Andor-Yokogawa-Leica spinning disc imaging system composed of an iXon3 electron-multiplying CCD camera and a computer-steered FRAP-PA (fluorescence recovery after photobleaching-photoactivation) device (56). Confocal images of the mid cross section of cells were acquired using a Leica HCX PL APO CS 63×/1.40 objective. Briefly, CFP was excited using 6-μW, 445-nm laser, and emission was collected using 478 ± 20 and 535 ± 20 filters.

Whole-cell recordings in HEK293 cells expressing various TRPs

HEK293 cells were grown as a monolayer in a 24-well plate using passage numbers less than 30 and maintained in Dulbecco's modified Eagle's medium (DMEM) (Life Technologies), supplemented with 10% fetal bovine serum (Life Technologies), penicillin (100 U/ml), and streptomycin (100 μg/ml) in a humidified incubator at 37°C with 5% CO_2. The cells were transiently transfected with 100-ng cDNA of mouse *Trpv4* (m*Trpv4*) and 100-ng cDNA of C1-GFP (green fluorescent protein), or 100-ng cDNA of mouse Trpv1 (m*Trpv1*) or 100-ng cDNA of mouse *Trpa1* (m*Trpa1*) using Lipofectamine 2000 (Invitrogen). After transfection, the cells were maintained in DMEM at 37°C for 24 hours before use.

Whole-cell patch-clamp recordings were performed using an EPC 10 amplifier (HEKA Elektronik) at room temperature (22° to 24°C) on the stage of an inverted phase-contrast

microscope equipped with a filter set for GFP visualization. Pipettes pulled from borosilicate glass (BF 150-86-10, Sutter Instrument) with a Sutter P-97 pipette puller had resistances of 2 to 4 megohms for whole-cell recordings, when filled with pipette solution containing 140 mM $CsCl_2$, 2 mM EGTA, and 10 mM Hepes, with pH 7.3 and 315 mOsm/liter in osmolarity. A Ca^{2+}-free extracellular solution was used for whole-cell recording to avoid Ca^{2+}-dependent desensitization of TRP channels, containing 140 mM NaCl, 5 mM KCl, 0.5 mM EGTA, 1 mM $MgCl_2$, 10 mM glucose, and 10 mM Hepes (pH was adjusted to 7.4 with NaOH, and the osmolarity was adjusted to ~340 mOsm/liter with sucrose). The whole-cell currents were recorded using voltage ramps from −100 to +100 mV during 500 ms at holding potential of 0 mV. Data were acquired using PATCHMASTER software (HEKA Elektronik). Currents were filtered at 2 kHz and digitized at 10 kHz. Data were analyzed and plotted using Clampfit 10 (Molecular Devices). The K_d values were calculated with the following function: $K_d = 100\ nM/(\tau_{off}/\tau_{on} - 1)$, where τ_{on} and τ_{off} are the fitted time constants for activation and washout of 100 nM capsaicin–activated currents (57, 58).

Statistical analyses

Values are reported as means ± SEM. Statistical analyses were performed using Prism 6 (version 6.0e, GraphPad). For comparison of the scratching responses of wild-type and *Trpv4*$^{-/-}$ mice, vehicle- and HC-treated mice, or control siRNA– and *Trpv4* siRNA–injected mice to CQ, histamine, or GSK101 (Fig. 2, A to C), a two-tailed unpaired *t* test was performed for each group. For comparison of control and *Trpv4* siRNA for mRNA abundance of *Trp* transcripts or TRPV4 protein abundance (Fig. 2, D and E), a two-tailed unpaired *t* test was performed for each group. For comparison of the GSK101-induced scratching responses of *Trpv4*$^{-/-}$, *Trpv1*$^{-/-}$, or *Trpa1*$^{-/-}$ to their respective wild-type littermates (Fig. 2F), a two-tailed unpaired *t* test was performed for each group. For comparison of CQ-and histamine-induced scratching responses of wild-type and *Trpv1*$^{-/-}$mice, mice treated with vehicle and SB, or mice injected with control and *Trpv1* siRNA (Fig. 3, A to C), a two-tailed unpaired *t* test was performed for each group. For comparison of the mRNA abundance of *Trp* transcripts or TRPV1 protein abundance in the DRG of control siRNA–and *Trpv1* siRNA–injected mice (Fig. 3, D and E), a two-tailed unpaired *t* test was performed for each group. For comparison of the scratching responses to histamine or CQ of the following mice—wild-type + control siRNA, *Trpv4*$^{-/-}$ + control siRNA, and *Trpv4*$^{-/-}$ + *Trpv1* siRNA (Fig. 3, F and G)—a one-way ANOVA followed by Newman-Keuls post hoc analysis was performed. For comparison of DRG responses from wild-type and *Trpv4*$^{-/-}$ mice or wild-type and *Trpv1*$^{-/-}$ mice to GSK101 or capsaicin from total DRG neurons (Fig. 4, B and E), a χ^2 test with Yates' correction was used. For comparison of first and second GSK101, CQ, or histamine responses in DRG of vehicle, HC, or SB groups (Fig. 4, G, I, and K), a two-tailed paired *t* test was performed for each group. For comparison of vehicle, HC 2.5, SB 2.5, HC 5, SB 5, and HC 2.5 + SB 2.5 treatments on scratching responses to CQ (Fig. 5A), a one-way ANOVA with Tukey post hoc analysis was performed. For comparison of GSK101, capsaicin, and GSK101 + capsaicin responses in DRG neurons responsive to both GSK101 and capsaicin (Fig. 5C), a one-way repeated-measures ANOVA with Tukey post hoc analysis was performed. For capsaicin and GSK101 + capsaicin responses in DRG neurons that were not responsive to GSK101 or capsaicin (Fig. 5D), a two-tailed paired *t* test was performed. For comparison of

pA/pF or K_d values in HEK293 cells expressing TRPV4, TRPV4 and TRPV1, and TRPV4 and TRPA1 (Fig. 8, D and F), a one-way ANOVA with Bonferroni post hoc analysis was performed for each group. For comparison of pA/pF or K_d values in HEK293 cells expressing TRPV1 and cells expressing TRPV1 and TRPV4 (Fig. 8, I and K), a two-tailed unpaired *t* test was performed. Comparisons passed normality and equal variance tests for use of parametric analyses. $P < 0.05$ was considered statistically significant.

Acknowledgments

We would like to thank G. Story for *Trpa1*$^{-/-}$ and *Trpv1*$^{-/-}$ mice, A. Patapoutian for TRPA1 antibody, X. Dong and Q. Liu for *Pirt-GCaMP3* mice, J. Yin for technical support, and the members of Chen's laboratory for comments.

Funding: The project has been supported by grants GM069027 and GM080558 to N.G., grants NS072377 and NSFC 31328011 to J.Z., and grant AR056318-01 to Z.-F.C. D.M.B. was supported by W.M. Keck Fellowship and NIH-NIDA T32 Training Grant (5T32DA007261-23).

REFERENCES AND NOTES

1. Clapham DE. TRP channels as cellular sensors. Nature. 2003; 426:517–524. [PubMed: 14654832]
2. Bandell M, Macpherson LJ, Patapoutian A. From chills to chilis: Mechanisms for thermosensation and chemesthesis via thermoTRPs. Curr Opin Neurobiol. 2007; 17:490–497. [PubMed: 17706410]
3. Bautista DM, Wilson SR, Hoon MA. Why we scratch an itch: The molecules, cells and circuits of itch. Nat Neurosci. 2014; 17:175–182. [PubMed: 24473265]
4. Basbaum AI, Bautista DM, Scherrer G, Julius D. Cellular and molecular mechanisms of pain. Cell. 2009; 139:267–284. [PubMed: 19837031]
5. Han SK, Simon MI. Intracellular signaling and the origins of the sensations of itch and pain. Sci Signal. 2011; 4:pe38. [PubMed: 21868356]
6. Bell JK, McQueen DS, Rees JL. Involvement of histamine H_4 and H_1 receptors in scratching induced by histamine receptor agonists in BalbC mice. Br J Pharmacol. 2004; 142:374–380. [PubMed: 15066908]
7. Osifo NG. Chloroquine-induced pruritus among patients with malaria. Arch Dermatol. 1984; 120:80–82. [PubMed: 6691718]
8. Liu Q, Tang Z, Surdenikova L, Kim S, Patel KN, Kim A, Ru F, Guan Y, Weng HJ, Geng Y, Undem BJ, Kollarik M, Chen ZF, Anderson DJ, Dong X. Sensory neuron-specific GPCR Mrgprs are itch receptors mediating chloroquine-induced pruritus. Cell. 2009; 139:1353–1365. [PubMed: 20004959]
9. Sun YG, Chen ZF. A gastrin-releasing peptide receptor mediates the itch sensation in the spinal cord. Nature. 2007; 448:700–703. [PubMed: 17653196]
10. Vandewauw I, Owsianik G, Voets T. Systematic and quantitative mRNA expression analysis of TRP channel genes at the single trigeminal and dorsal root ganglion level in mouse. BMC Neurosci. 2013; 14:21. [PubMed: 23410158]
11. Akiyama T, Ivanov M, Nagamine M, Davoodi A, Carstens MI, Ikoma A, Cevikbas F, Kempkes C, Buddenkotte J, Steinhoff M, Carstens E. Involvement of TRPV4 in serotonin-evoked scratching. J Invest Dermatol. 2015; 136:154–160.
12. Roberson DP, Gudes S, Sprague JM, Patoski HAW, Robson VK, Blasl F, Duan B, Oh SB, Bean BP, Ma Q, Binshtok AM, Woolf CJ. Activity-dependent silencing reveals functionally distinct itch-generating sensory neurons. Nat Neurosci. 2013; 16:910–918. [PubMed: 23685721]
13. Imamachi N, Park GH, Lee H, Anderson DJ, Simon MI, Basbaum AI, Han SK. TRPV1-expressing primary afferents generate behavioral responses to pruritogens via multiple mechanisms. Proc Natl Acad Sci USA. 2009; 106:11330–11335. [PubMed: 19564617]

14. Shim WS, Tak MH, Lee MH, Kim M, Kim M, Koo JY, Lee CH, Kim M, Oh U. TRPV1 mediates histamine-induced itching via the activation of phospholipase A_2 and 12-lipoxygenase. J Neurosci. 2007; 27:2331–2337. [PubMed: 17329430]
15. Wilson SR, Gerhold KA, Bifolck-FIsher A, Liu Q, Patel KN, Dong X, Bautista DM. TRPA1 is required for histamine-independent, Mas-related G protein–coupled receptor–mediated itch. Nat Neurosci. 2011; 14:595–602. [PubMed: 21460831]
16. Than JY-XL, Li L, Hasan R, Zhang X. Excitation and modulation of TRPA1, TRPV1, and TRPM8 channel-expressing sensory neurons by the pruritogen chloroquine. J Biol Chem. 2013; 288:12818–12827. [PubMed: 23508958]
17. Han L, Ma C, Liu Q, Weng HJ, Cui Y, Tang Z, Kim Y, Nie H, Qu L, Patel KN, Li Z, McNeil B, He S, Guan Y, Xiao B, LaMotte RH, Dong X. A subpopulation of nociceptors specifically linked to itch. Nat Neurosci. 2013; 16:174–182. [PubMed: 23263443]
18. Suzuki M, Mizuno A, Kodaira K, Imai M. Impaired pressure sensation in mice lacking TRPV4. J Biol Chem. 2003; 278:22664–22668. [PubMed: 12692122]
19. Everaerts W, Zhen X, Ghosh D, Vriensa J, Gevaert T, Gilbert JP, Hayward NJ, McNamara CR, Xue F, Moran MM, Strassmaier T, Uykal E, Owsianik G, Vennekens R, De Ridder D, Nilius B, Fanger CM, Voets T. Inhibition of the cation channel TRPV4 improves bladder function in mice and rats with cyclophosphamide-induced cystitis. Proc Natl Acad Sci USA. 2010; 107:19084–19089. [PubMed: 20956320]
20. Chung MK, Lee H, Mizuno A, Suzuki M, Caterina MJ. TRPV3 and TRPV4 mediate warmth-evoked currents in primary mouse keratinocytes. J Biol Chem. 2004; 279:21569–21575. [PubMed: 15004014]
21. Alexander R, Kerby A, Aubdool AA, Power AR, Grover S, Gentry C, Grant AD. 4α-phorbol 12,13-didecanoate activates cultured mouse dorsal root ganglia neurons independently of TRPV4. Br J Pharmacol. 2013; 168:761–772. [PubMed: 22928864]
22. Thorneloe KS, Sulpizio AC, Lin Z, Figueroa DJ, Clouse AK, McCafferty GP, Chendrimada TP, Lashinger ESR, Gordon E, Evans L, Misajet BA, DeMarini DJ, Nation JH, Casillas LN, Marquis RW, Votta BJ, Sheardown SA, Xu X, Brooks DP, Laping NJ, Westfall TD. N-((1S)-1-{[4-((2S)-2-{[(2,4-dichlorophenyl)sulfonyl]amino}-3-hydroxypropanoyl)-1-piperazinyl]carbonyl}-3-methylbutyl)-1-benzothiophene-2-carboxamide (GSK1016790A), a novel and potent transient receptor potential vanilloid 4 channel agonist induces urinary bladder contraction and hyperactivity: Part I. J Pharmacol Exp Ther. 2008; 326:432–442. [PubMed: 18499743]
23. Kwan KY, Allchorne AJ, Vollrath MA, Christensen AP, Zhang D-S, Woolf CJ, Corey DP. TRPA1 contributes to cold, mechanical, and chemical nociception but is not essential for hair-cell transduction. Neuron. 2006; 50:277–289. [PubMed: 16630838]
24. Caterina MJ, Leffler A, Malmberg AB, Martin WJ, Trafton J, Petersen-Zeitz KR, Koltzenburg M, Basbaum AI, Julius D. Impaired nociception and pain sensation in mice lacking the capsaicin receptor. Science. 2000; 288:306–313. [PubMed: 10764638]
25. Patapoutian A, Tate S, Woolf CJ. Transient receptor potential channels: Targeting pain at the source. Nat Rev Drug Discov. 2009; 8:55–68. [PubMed: 19116627]
26. Sharif-Naeini R, Ciura S, Bourque CW. *TRPV1* gene required for thermosensory transduction and anticipatory secretion from vasopressin neurons during hyperthermia. Neuron. 2008; 58:179–185. [PubMed: 18439403]
27. Gunthorpe MJ, Rami HK, Jerman JC, Smart D, Gill CH, Soffin EM, Luis Hannan S, Lappin SC, Egerton J, Smith GD, Worby A, Howett L, Owen D, Nasir S, Davies CH, Thompson M, Wyman PA, Randall AD, Davis JB. Identification and characterisation of SB-366791, a potent and selective vanilloid receptor (VR1/TRPV1) antagonist. Neuropharmacology. 2004; 46:133–149. [PubMed: 14654105]
28. Kim YS, Chu Y, Han L, Li M, Li Z, LaVinka PC, Sun S, Tang Z, Park K, Caterina MJ, Ren K, Dubner R, Wei F, Dong X. Central terminal sensitization of TRPV1 by descending serotonergic facilitation modulates chronic pain. Neuron. 2014; 81:837–887.
29. Akiyama T, Tominaga M, Davoodi A, Nagamine M, Blansit K, Horwitz A, Carstens MI, Carstens E. Cross-sensitization of histamine-independent itch in mouse primary sensory neurons. Neuroscience. 2012; 226:305–312. [PubMed: 23000623]

30. Takanishi CL, Bykova EA, Cheng W, Zheng J. GFP-based FRET analysis in live cells. Brain Res. 2006; 1091:132–139. [PubMed: 16529720]

31. Cheng W, Yang F, Takanishi CL, Zheng J. Thermosensitive TRPV channel subunits coassemble into heteromeric channels with intermediate conductance and gating properties. J Gen Physiol. 2007; 129:191–207. [PubMed: 17325193]

32. Willette RN, Bao W, Nerurkar S, Yue T-l, Doe CP, Stankus G, Turner GH, Ju H, Thomas H, Fishman CE, Sulpizio A, Behm DJ, Hoffman S, Lin Z, Lozinskaya I, Casillas LN, Lin M, Trout REL, Votta BJ, Thorneloe K, Lashinger ESR, Figueroa DJ, Marquis R, Xu X. Systemic activation of the transient receptor potential vanilloid subtype 4 channel causes endothelial failure and circulatory collapse: Part 2. J Pharmacol Exp Ther. 2008; 326:443–452. [PubMed: 18499744]

33. Davis JB, Gray J, Gunthorpe MJ, Hatcher JP, Davey PT, Overend P, Harries MH, Latcham J, Clapham C, Atkinson K, Hughes SA, Rance K, Grau E, Harper AJ, Pugh PL, Rogers DC, Bingham S, Randall A, Sheardown SA. Vanilloid receptor-1 is essential for inflammatory thermal hyperalgesia. Nature. 2000; 405:183–187. [PubMed: 10821274]

34. Cui M, Honore P, Zhong C, Gauvin D, Mikusa J, Hernandez G, Chandran P, Gomtsyan A, Brown B, Bayburt EK, Marsh K, Bianchi B, McDonald H, Niforatos W, Neelands TR, Moreland RB, Decker MW, Lee CH, Sullivan JP, Faltynek CR. TRPV1 receptors in the CNS play a key role in broad-spectrum analgesia of TRPV1 antagonists. J Neurosci. 2006; 26:9385–9393. [PubMed: 16971522]

35. Kim YH, Back SK, Davies AJ, Jeong H, Jo HJ, Chung G, Na HS, Bae YC, Kim SJ, Kim JS, Jung SJ, Oh SB. TRPV1 in GABAergic interneurons mediates neuropathic mechanical allodynia and disinhibition of the nociceptive circuitry in the spinal cord. Neuron. 2012; 74:640–647. [PubMed: 22632722]

36. Liedtke W, Friedman JM. Abnormal osmotic regulation in *trpv4*$^{-/-}$ mice. Proc Natl Acad Sci USA. 2003; 100:13698–13703. [PubMed: 14581612]

37. Phelps CB, Wang RR, Choo SS, Gaudet R. Differential regulation of TRPV1, TRPV3, and TRPV4 sensitivity through a conserved binding site on the ankyrin repeat domain. J Biol Chem. 2010; 285:731–740. [PubMed: 19864432]

38. Auer-Grumbach M, Olschewski A, Papić L, Kremer H, McEntagart ME, Uhrig S, Fischer C, Fröhlich E, Bálint Z, Tang B, Strohmaier H, Lochmüller H, Schlotter-Weigel B, Senderek J, Krebs A, Dick KJ, Petty R, Longman C, Anderson NE, Padberg GW, Schelhaas HJ, van Ravenswaaij-Arts CMA, Pieber TR, Crosby AH, Guelly C. Alterations in the ankyrin domain of TRPV4 cause congenital distal SMA, scapuloperoneal SMA and HMSN2C. Nat Genet. 2010; 42:160–164. [PubMed: 20037588]

39. Poole DP, Amadesi S, Veldhuis NA, Abogadie FC, Lieu T, Darby W, Liedtke W, Lew MJ, McIntyre P, Bunnett NW. Protease-activated receptor 2 (PAR_2) protein and transient receptor potential vanilloid 4 (TRPV4) protein coupling is required for sustained inflammatory signaling. J Biol Chem. 2013; 288:5790–5802. [PubMed: 23288842]

40. Chen Y, Yang C, Wang ZJ. Proteinase-activated receptor 2 sensitizes transient receptor potential vanilloid 1, transient receptor potential vanilloid 4, and transient receptor potential ankyrin 1 in paclitaxel-induced neuropathic pain. Neuroscience. 2011; 193:440–451. [PubMed: 21763756]

41. Grant AD, Cottrell GS, Amadesi S, Trevisani M, Nicoletti P, Materazzi S, Altier C, Cenac N, Zamponi GW, Bautista-Cruz F, Lopez CB, Joseph EK, Levine JD, Liedtke W, Vanner S, Vergnolle N, Geppetti P, Bunnett NW. Protease-activated receptor 2 sensitizes the transient receptor potential vanilloid 4 ion channel to cause mechanical hyperalgesia in mice. J Physiol. 2007; 578:715–733. [PubMed: 17124270]

42. Sudbury JR, Bourque CW. Dynamic and permissive roles of TRPV1 and TRPV4 channels for thermosensation in mouse supraoptic magnocellular neurosecretory neurons. J Neurosci. 2013; 33:17160–17165. [PubMed: 24155319]

43. Lishko PV, Procko E, Jin X, Phelps CB, Gaudet R. The ankyrin repeats of TRPV1 bind multiple ligands and modulate channel sensitivity. Neuron. 2007; 54:905–918. [PubMed: 17582331]

44. Köttgen M, Buchholz B, Garcia-Gonzalez MA, Kotsis F, Fu X, Doerken M, Boehlke C, Steffl D, Tauber R, Wegierski T, Nitschke R, Suzuki M, Kramer-Zucker A, Germino GG, Watnick T, Prenen J, Nilius B, Kuehn EW, Walz G. TRPP2 and TRPV4 form a polymodal sensory channel complex. J Cell Biol. 2008; 182:437–447. [PubMed: 18695040]

45. Stewart AP, Smith GD, Sandford RN, Edwardson JM. Atomic force microscopy reveals the alternating subunit arrangement of the TRPP2-TRPV4 heterotetramer. Biophys J. 2010; 99:790–797. [PubMed: 20682256]
46. Alessandri-Haber N, Dina OA, Chen X, Levine JD. TRPC1 and TRPC6 channels cooperate with TRPV4 to mediate mechanical hyperalgesia and nociceptor sensitization. J Neurosci. 2009; 29:6217–6228. [PubMed: 19439599]
47. Tobin DM, Madsen DM, Kahn-Kirby A, Peckol EL, Moulder G, Barstead R, Maricq AV, Bargmann CI. Combinatorial expression of TRPV channel proteins defines their sensory functions and subcellular localization in *C. elegans* neurons. Neuron. 2002; 35:307–318. [PubMed: 12160748]
48. Zhao ZQ, Scott M, Chiechio S, Wang J-S, Renner KJ, Gereau RW IV, Johnson RL, Deneris ES, Chen Z-F. *Lmx1b* is required for maintenance of central serotonergic neurons and mice lacking central serotonergic system exhibit normal locomotor activity. J Neurosci. 2006; 26:12781–12788. [PubMed: 17151281]
49. Sharif Naeini R, Witty M-F, Séguéla P, Bourque CW. An N-terminal variant of Trpv1 channel is required for osmosensory transduction. Nat Neurosci. 2006; 9:93–98. [PubMed: 16327782]
50. Schmidt M, Dubin AE, Petrus MJ, Earley TJ, Patapoutian A. Nociceptive signals induce trafficking of TRPA1 to the plasma membrane. Neuron. 2009; 64:498–509. [PubMed: 19945392]
51. Liu XY, Wan L, Huo FQ, Barry DM, Li H, Zhao ZQ, Chen ZF. B-type natriuretic peptide is neither itch-specific nor functions upstream of the GRP-GRPR signaling pathway. Mol Pain. 2014; 10:4. [PubMed: 24438367]
52. Zhao ZQ, Wan L, Liu XY, Huo FQ, Li H, Barry DM, Krieger S, Kim S, Liu ZC, Xu J, Rogers BE, Li YQ, Chen ZF. Cross-inhibition of NMBR and GRPR signaling maintains normal histaminergic itch transmission. J Neurosci. 2014; 34:12402–12414. [PubMed: 25209280]
53. Liu XY, Liu ZC, Sun YG, Ross M, Kim S, Tsai FF, Li QF, Jeffry J, Kim JY, Loh HH, Chen ZF. Unidirectional cross-activation of GRPR by MOR1D uncouples itch and analgesia induced by opioids. Cell. 2011; 147:447–458. [PubMed: 22000021]
54. Berrout J, Jin M, Mamenko M, Zaika O, Pochynyuk O, O'Neil RG. Function of transient receptor potential cation channel subfamily V member 4 (TRPV4) as a mechanical transducer in flow-sensitive segments of renal collecting duct system. J Biol Chem. 2012; 287:8782–8791. [PubMed: 22298783]
55. Zheng J, Trudeau MC, Zagotta WN. Rod cyclic nucleotide-gated channels have a stoichiometry of three CNGA1 subunits and one CNGB1 subunit. Neuron. 2002; 36:891–896. [PubMed: 12467592]
56. Karunarathne WKA, Giri L, Kalyanaraman V, Gautam N. Optically triggering spatiotemporally confined GPCR activity in a cell and programming neurite initiation and extension. Proc Natl Acad Sci USA. 2013; 110:E1565–E1574. [PubMed: 23479634]
57. Saito M, Nelson C, Salkoff L, Lingle CJ. A cysteine-rich domain defined by a novel exon in *aSlo* variant in rat adrenal chromaffin cells and PC12 cells. J Biol Chem. 1997; 272:11710–11717. [PubMed: 9115223]
58. Gan G, Yi H, Chen M, Sun L, Li W, Wu Y, Ding J. Structural basis for toxin resistance of β4-associated calcium-activated potassium (BK) channels. J Biol Chem. 2008; 283:24177–24184. [PubMed: 18559348]

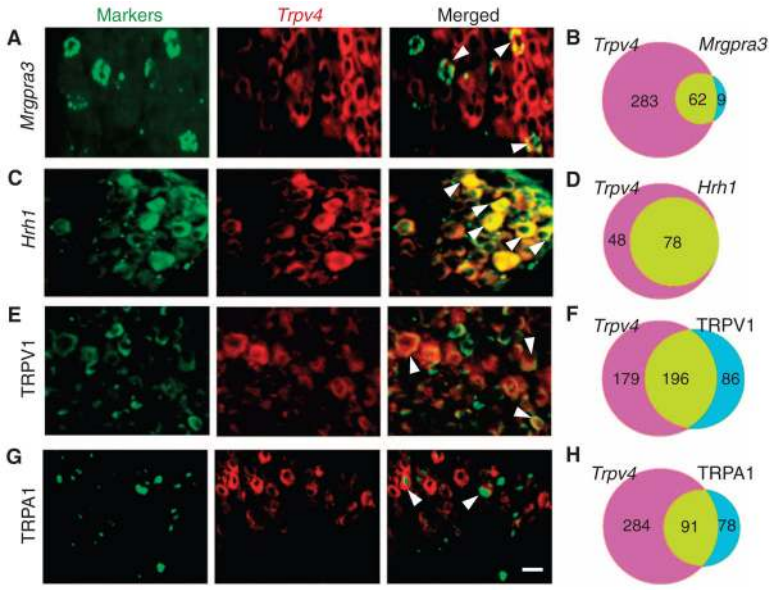

Fig. 1. TRPV4 is expressed in itch-sensing sensory neurons

(**A** and **B**) Images of the double fluorescence in situ hybridization of *Trpv4* and *Mrgpra3* in mouse-dissociated DRG neurons and a Venn diagram of the number of the overlap. (**C** and **D**) Double fluorescence in situ hybridization of *Hrh1* and *Trpv4* in mouse dissociated DRG neurons and a Venn diagram of the overlap. (**E** to **H**) In situ hybridization of *Trpv4* followed by TRPV1 immunohistochemistry (E) or TRPA1 immunohistochemistry (G) and Venn diagrams of the overlap between *Trpv4* and TRPV1 (F) or *Trpv4* and TRPA1 (H) in DRG neurons. $n = 3$ mice and 10 sections per in situ hybridization and immunohistochemistry experiment. Scale bar, 20 μm. Arrowheads, double-stained neurons.

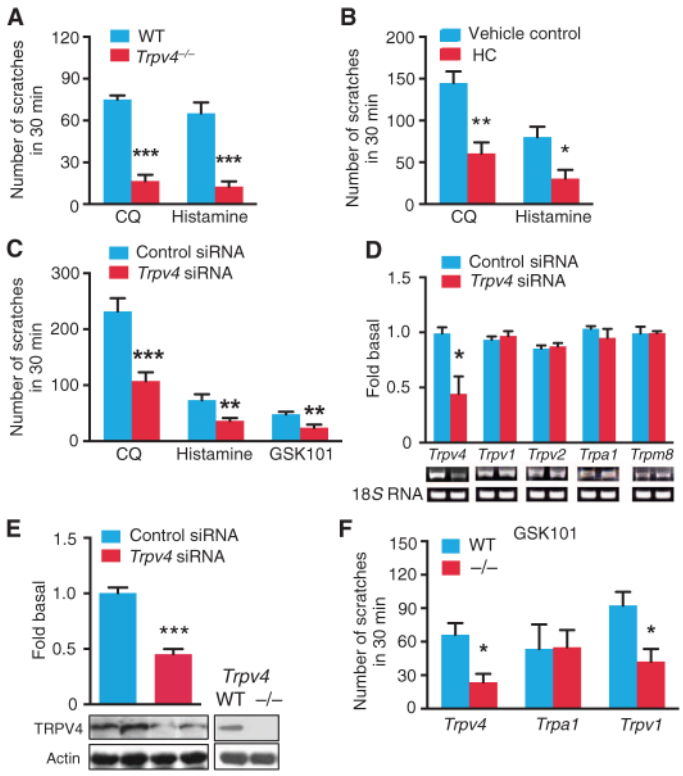

Fig. 2. TRPV4 is a mediator of both CQ- and histamine-induced itch

(**A**) Scratching responses induced by intradermal injection of CQ (200 μg) and histamine (200 μg) in *Trpv4*$^{-/-}$ mice and wild-type (WT) littermates. (**B**) Scratching responses in WT mice preinjected (intraperitoneal) with vehicle control (2% DMSO) or TRPV4 antagonist HC (10 mg/kg) followed by CQ (200 μg) or histamine (200 μg). (**C**) Scratching responses to intradermal CQ (200 μg), histamine (200 μg), or GSK101 (10 μg) in mice intrathecally injected with control siRNA or *Trpv4* siRNA. (**D**) Quantitative reverse transcription polymerase chain reaction (qRT-PCR) of the indicated TRP family member transcripts in DRG of control siRNA– or *Trpv4* siRNA–injected mice. Fold basal was determined by normalizing the data to control siRNA group. (**E**) Western blot of TRPV4 in DRG of control siRNA– or *Trpv4* siRNA–injected mice. Fold basal was determined by normalizing the data to WT group. Validation of the antibody using DRG from *Trpv4*$^{-/-}$ mice. (**F**) Scratching response induced by intradermal injection of GSK101 (10 μg) in *Trpv4*$^{-/-}$, *Trpv1*$^{-/-}$, and *Trpa1*$^{-/-}$ mice and their respective WT littermates. Data are means ± SEM, and error bars represent SEM. **P* < 0.05, ***P* < 0.01, ****P* < 0.001, unpaired *t* test; *n* = 6 to 8 mice for behavior, and *n* = 4 for RT-PCR and Western blots.

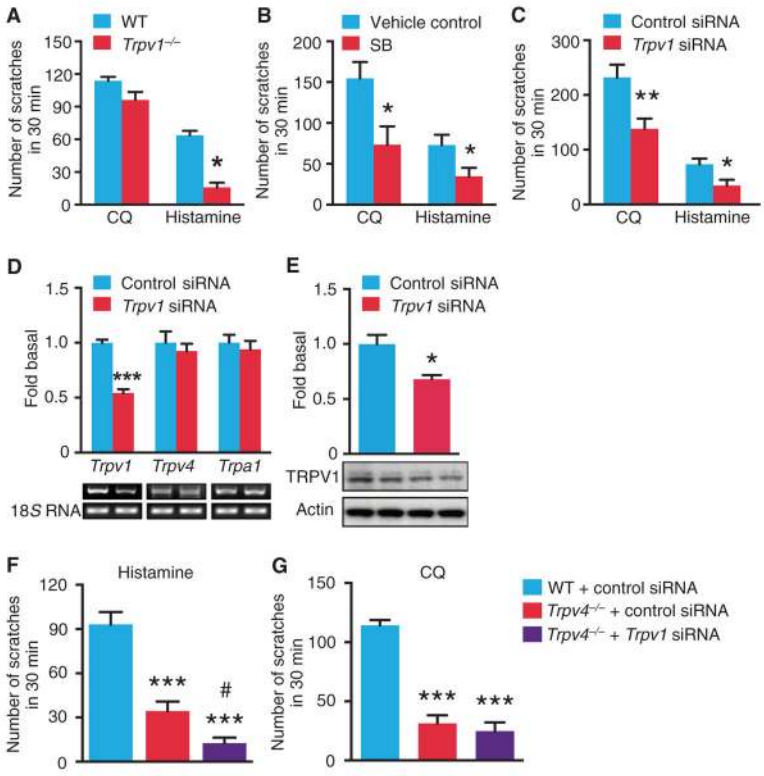

Fig. 3. TRPV1 facilitates CQ-induced itch

(**A**) Scratching responses of WT and *Trpv1*$^{-/-}$ litter-mates to CQ and histamine. (**B**) Scratching responses to CQ and histamine in WT mice after intraperitoneal preinjection of vehicle control (2% DMSO) or TRPV1 antagonist SB (10 mg/kg). (**C**) Scratching responses to CQ and histamine in control siRNA– and *Trpv1* siRNA–injected mice. (**D**) qRT-PCR of the indicated TRP family member transcripts in DRG of control siRNA–and *Trpv1* siRNA–injected mice. (**E**) Western blot of TRPV1 in DRG of control siRNA– and *Trpv1* siRNA–injected mice. (**F** and **G**) Scratching responses to histamine (F) and CQ (G) in control siRNA–injected WT, control siRNA–injected *Trpv4*$^{-/-}$, and *Trpv1* siRNA–injected *Trpv4*$^{-/-}$ mice. Data are means ± SEM, and error bars represent SEM. *$P < 0.05$, **$P < 0.01$, ***$P < 0.001$ versus control in (B) and (E), versus WT in (A), (F), and (G); $^{\#}P < 0.05$ versus *Trpv4*$^{-/-}$ in (F); unpaired *t* test in (A) to (E); one-way analysis of variance (ANOVA) with Newman-Keuls post hoc in (F) and (G). $n = 6$ to 8 mice for behavior, and $n = 4$ for RT-PCR and Western blots.

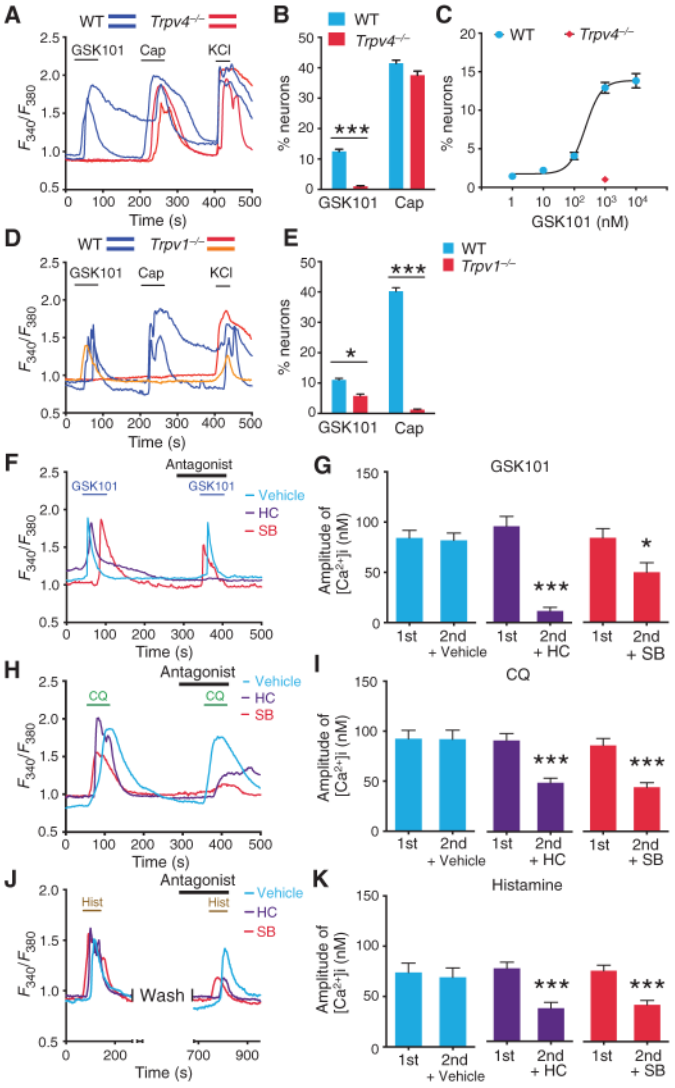

Fig. 4. GSK101 is a specific agonist for TRPV4, and antagonism of TRPV4 or TRPV1 inhibits CQ- and histamine-induced Ca^{2+} signaling in sensory neurons

(**A**) Representative traces showing Ca^{2+} responses of cultured DRG neurons from WT and *Trpv4*$^{-/-}$ during application of GSK101 (1 μM), capsaicin (Cap; 100 nM), or KCl (30 mM). (**B**) GSK101-responsive neurons as a percentage of total KCl-responsive DRG neurons from WT (104 of 841, 13%) and *Trpv4*$^{-/-}$ (10 of 937, 1%) mice and the percentage of capsaicin-responsive DRG neurons from WT (345 of 841, 42%) and *Trpv4*$^{-/-}$ (351 of 937, 38%) mice. (**C**) Dose response of DRG neurons from WT and *Trpv4*$^{-/-}$DRG neurons to GSK101. (**D**) Representative traces showing Ca^{2+} responses of cultured DRG neurons from WT and *Trpv1*$^{-/-}$ mice during application of GSK101, capsaicin, or KCl. Concentrations are same as in (A). (**E**) GSK101-responsive neurons as a percentage of total KCl-responsive DRG neurons from WT (147 of 1323, 11%) and *Trpv1*$^{-/-}$ (75 of 1254, 6%) mice and the percentage of capsaicin-responsive DRG neurons from WT (530 of 1323, 40%) and *Trpv1*$^{-/-}$ (15 of 1254, 1%) mice. (**F**) Representative traces showing Ca^{2+} responses of GSK101-responsive cultured DRG neurons that responded to GSK101 (1 μM) coapplied

with vehicle (0.1% DMSO), HC (10 μM), or SB (10 μM). After first application of GSK101 and washout, antagonists or vehicle control was preapplied for 1 min and coapplied with a second GSK101. (**G**) Amplitudes of $[Ca^{2+}]_i$ responses from first and second GSK101 applications in control, HC-treated, or SB-treated DRG neurons. (**H**) Representative traces showing Ca^{2+} responses of CQ (1 mM)–responsive DRG neurons that responded to CQ coapplied with vehicle (0.1% DMSO), HC (10 μM), or SB (10 μM). (**I**) Amplitudes of $[Ca^{2+}]_i$ responses from first and second CQ applications in control, HC-treated, or SB-treated DRG neurons. (**J**) Representative traces showing Ca^{2+} responses of histamine (Hist) (50 μM)–responsive DRG neurons that responded to histamine co-applied with vehicle (0.1% DMSO), HC (10 μM), or SB (10 μM). (**K**) Amplitudes of $[Ca^{2+}]_i$ responses from first and second histamine applications in control, HC-treated, or SB-treated DRG neurons. Data are means ± SEM, and error bars represent SEM. $*P < 0.05$, $***P < 0.001$, χ^2 test with Yates' correction in (B) and (E), paired *t* test in (G), (I), and (K). $n = 3$ to 4 mice, and ~100 DRG neurons were examined for each mouse.

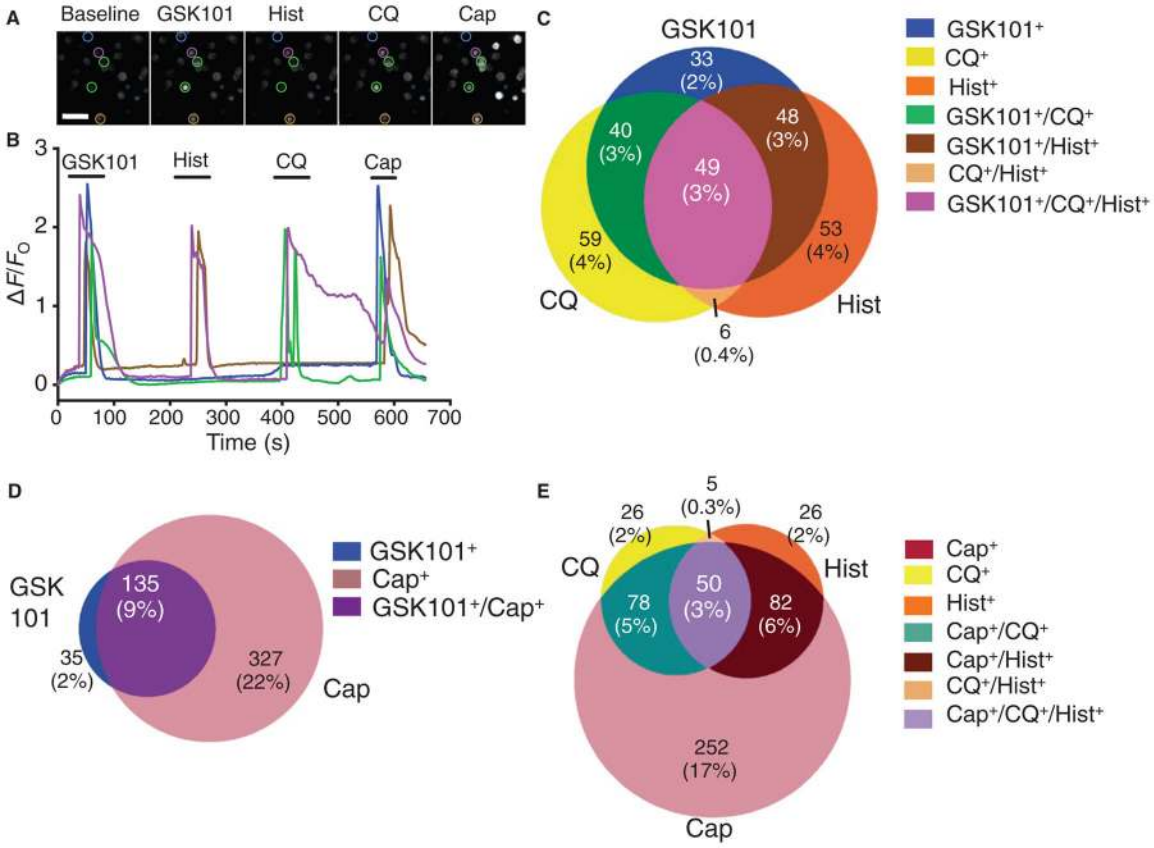

Fig. 5. Most of the CQ- and histamine-responsive neurons respond to the TRPV4 agonist GSK101

(**A**) $[Ca^{2+}]_i$ responses in *Pirt-GCaMP3* DRG neurons during application of GSK101 (1 μM), histamine (50 μM), CQ (1 mM), or capsaicin (100 nM). Blue circles, neurons responsive to GSK101 and capsaicin; violet circles, neurons responsive to GSK101, histamine, CQ, and capsaicin; brown circles, neurons responsive to GSK101, histamine, and capsaicin; green circles, neurons responsive to GSK101, CQ, and capsaicin. (**B**) Representative traces for neurons that respond to GSK101 and capsaicin (blue); GSK101, histamine, CQ, and capsaicin (violet); GSK101, histamine, and capsaicin (brown); or GSK101, CQ, and capsaicin (green). (**C**) Venn diagram of DRG neurons responsive to GSK101, histamine, and CQ. (**D**) Venn diagram of DRG neurons responsive to GSK101 and capsaicin. (**E**) Venn diagram of DRG neurons responsive to capsaicin, histamine, and CQ. Number and percentage of total neurons that were responsive are indicated for each group. Scale bar, 100 μm. $n = 4$ mice per group.

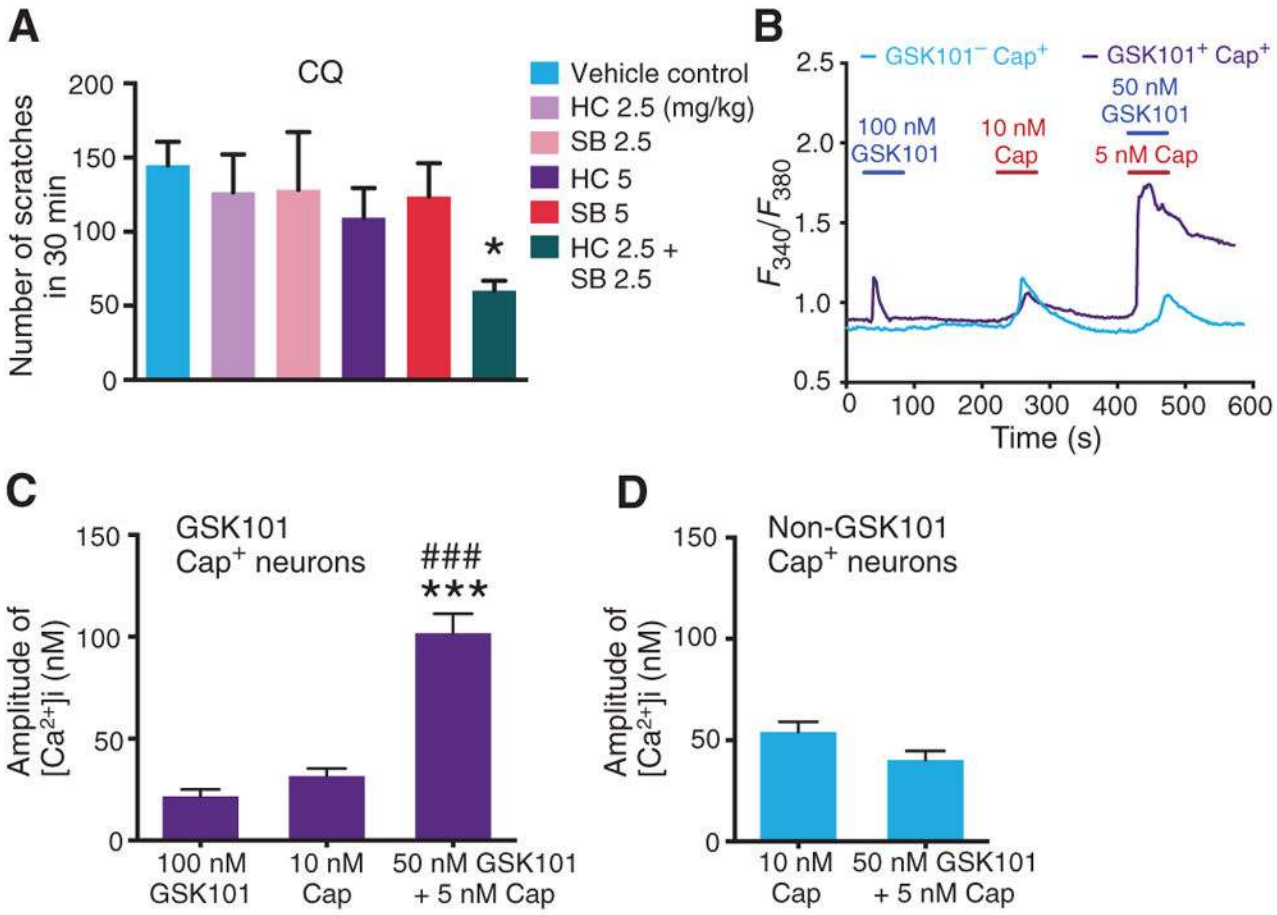

Fig. 6. TRPV1 facilitates TRPV4-mediated itch

(**A**) Scratching responses to CQ in mice intraperitoneally preinjected with vehicle control (XXX), HC, SB, or the indicated combinations at the indicated concentrations. (**B**) Representative traces showing Ca^{2+} responses in DRG neurons during exposure to 100 nM GSK101 and 10 nM capsaicin, or coapplication of 50 nM GSK101 and 5 nM capsaicin. (**C** and **D**) Amplitude of $[Ca^{2+}]_i$ responses in DRG neurons that are GSK101-responsive (C) or in DRG neurons that do not respond to GSK101 (non-GSK101) (D) exposed to 100 nM GSK101 and 10 nM capsaicin, or coapplication of 50 nM GSK101 and 5 nM capsaicin. Data are means ± SEM, and error bars represent SEM. $^{*}P < 0.05$ versus control, $^{***}P < 0.001$ versus GSK101, $^{\#\#\#}P < 0.001$ versus capsaicin, one-way ANOVA with Tukey post hoc in (A), one-way repeated-measures ANOVA with Tukey post hoc in (C), and paired *t* tests in (D). $n = 6$ to 8 mice for behavior, $n = 3$ to 4 mice for Ca^{2+} responses, and ~100 DRG neurons were examined for each mouse.

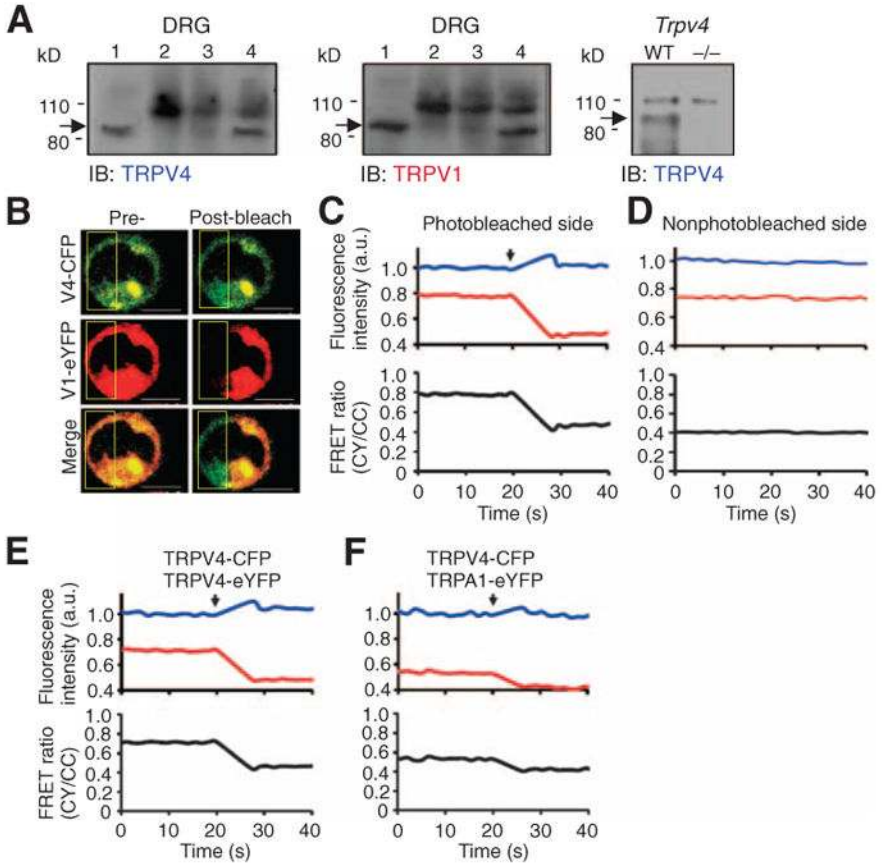

Fig. 7. TRPV4 and TRPV1 form complexes in DRG neurons and HEK293 cells

(**A**) Coimmunoprecipitation of TRPV4 and TRPV1 from DRG membrane preparations from WT or *Trpv4*$^{-/-}$ mice. Rabbit antibody (1 μg) recognizing TRPV4 was used for immunoprecipitation, and proteins were blotted (IB) with antibodies recognizing either TRPV4 or TRPV1. Left and middle: Input to show abundance of TRPV4 and TRPV1 (arrows) in the DRG preparations (lane 1); immunoprecipitation with an irrelevant rabbit IgG (lane 2); phosphate-buffered saline (PBS) control in which DRG membrane proteins were omitted (lane 3); proteins immunoprecipitated from DRG membranes with the antibody recognizing TRPV4 (lane 4). Right: Immunoprecipitation with the antibody recognizing TRPV4 from DRG membrane preparations from WT and *Trpv4*$^{-/-}$ (–/–) mice. (**B**) Representative confocal images showing plasma membrane fluorescence intensities of HEK293 cells expressing TRPV4-CFP (V4-CFP) and TRPV1-eYFP (V1-eYFP), before and after acceptor (eYFP) photobleaching in the selected region of a cell (yellow boxes). Overlaid images show typical example of a cell coexpressing TRPV4-CFP and TRPV1-eYFP. Scale bars, 10 μm. (**C**) Top: Background-subtracted, normalized fluorescence intensities of donor emission (blue trace, 445-nm excitation/478-nm emission; CC) and acceptor emission (red trace, 445-nm excitation/515-nm emission; CY) from selected plasma membrane regions [yellow boxes in (B)]. Bottom: FRET ratio (CY/CC) of the photobleached regions [yellow boxes in (B)]. a.u., arbitrary units. (**D**) Fluorescence intensities (top) and FRET ratio (bottom) of nonphotobleached regions. (**E** and **F**) Acceptor photobleaching FRET of cells expressing TRPV4-CFP and TRPV4-eYFP (E) and cells

expressing TRPV4-CFP and TRPA1-eYFP (F). Arrows indicate photobleaching at 20 s. Data are representative of 3 experiments.

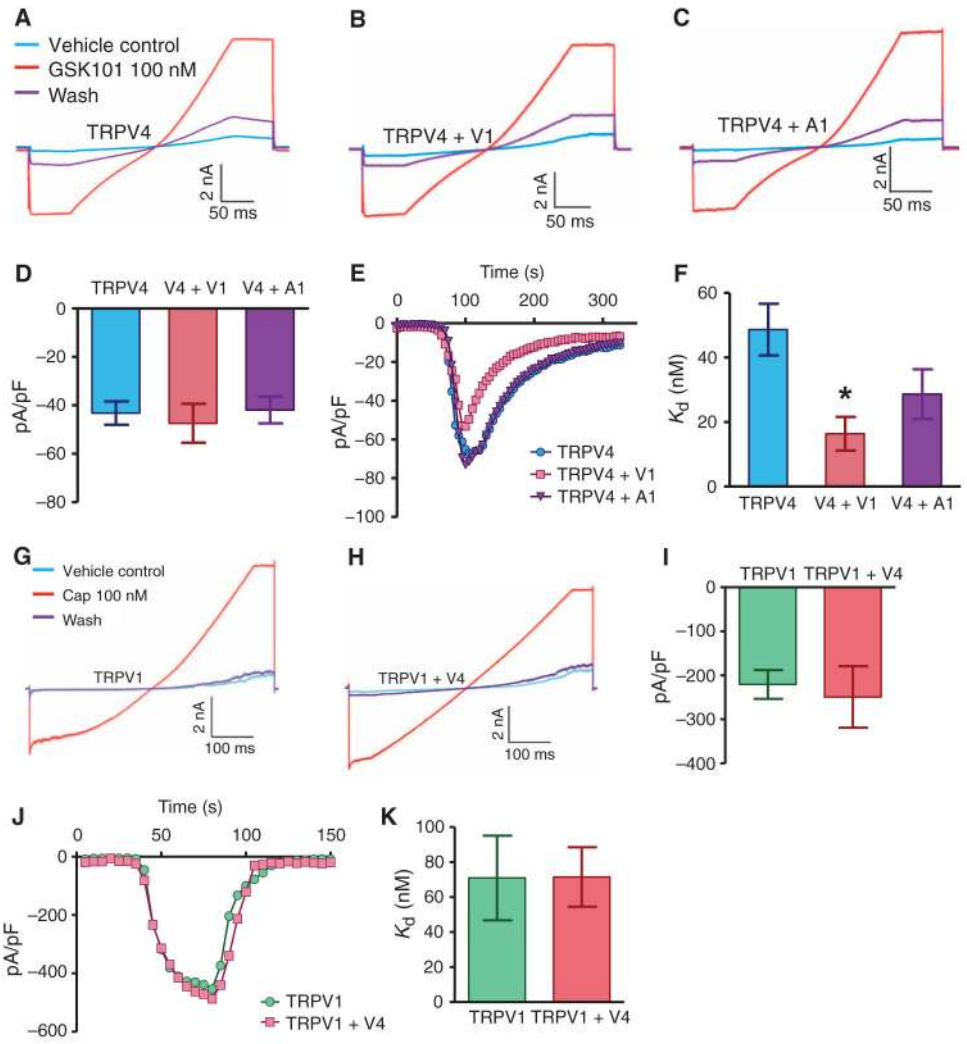

Fig. 8. TRPV1 facilitates TRPV4 activation in HEK293 cells

(**A** to **C**) Representative current traces activated by 100 nM GSK101 in cells expressing the indicated TRP channels. Traces for the vehicle control response, the GSK101 response, and the activity after washout of the GSK101 are shown. Data are representative of 7 to 9 cells. (**D**) Bar graph shows the averaged current density activated by 100 nM GSK101 in cells expressing the indicated TRP channels. Data are means ± SEM; $n = 5$ to 9 cells in 3 experiments. (**E**) Representative time courses of 100 nM GSK101–activated currents in cells expressing the indicated TRP channels. Solid lines show the activation, and washout kinetics fit to a single exponential function. (**F**) K_d's of GSK101 for TRPV4 alone or in the presence of the TRPV1 or TRPA1. (**G** and **H**) Representative current traces activated by 100 nM capsaicin in cells expressing TRPV1 (G) or TRPV1 and TRPV4 (H). Data are representative of 10 cells. (**I**) Bar graph shows the averaged current density activated by 100 nM capsaicin in cells expressing the indicted TRP channels. Data are means ± SEM. (**J**) Representative time courses of 100 nM capsaicin–activated currents in cells expressing TRPV1 alone or TRPV1 and TRPV4. Data are representative of 10 cells. (**K**) K_d of capsaicin for TRPV1 alone or in the presence of TRPV4. Data are means ± SEM, and error bars represent SEM.

In (F) and (K), $*P < 0.05$ versus TRPV4 or TRPV1 alone, one-way ANOVA with Bonferroni post hoc test. The K_d values were calculated with the following function: $K_d = 100\ nM/(\tau_{off}/\tau_{on} - 1)$, where τ_{on} and τ_{off} are the fitted time constants for activation and washout of 100 nM GSK101–activated currents. V1, TRPV1; V4, TRPV4; A1, TRPA1.

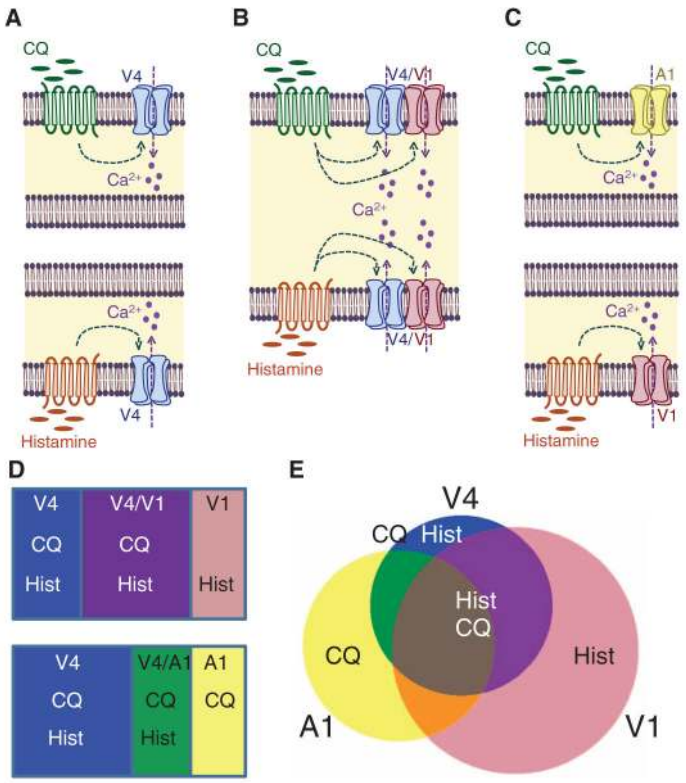

Fig. 9. Models of the roles of TRP channels in CQ- and histamine-induced itch signaling in sensory neurons

(**A**) CQ- and histamine-induced itch are mediated by distinct TRPV4-positive populations of DRG neurons that lack TRPV1. (**B**) CQ- and histamine-induced itch are mediated by a subset of neurons that have both TRPV1 and TRPV4, which form functional complexes. (**C**) CQ-induced itch is mediated by TRPA1-positive neurons, whereas histamine-induced itch is mediated by TRPV1-positive neurons. (**D**) Diagrams showing the overlap of TRPV4 with TRPV1 (upper panel) or TRPV4 with TRPA1 (lower panel) and their respective roles in CQ- and histamine-induced itch signaling. (**E**) Venn diagram indicating overlapping activity of TRPV4 with TRPV1 or TRPA1 based on Ca^{2+} imaging studies. V1, TRPV1-positive neurons; V4, TRPV4-positive neurons; V4/V1, neurons positive for both TRPV4 and TRPV1; A1, TRPA1-positive neurons; V4/A1, neurons positive for both TRPV4 and TRPA1.

Table 1

FRET between TRPV4-CFP and the indicated eYFP-tagged TRP channel expressed in HEK293 cells

The FRET efficiency value is determined by fitting the FRET model to each coexpression experiment and is given as a percentage as described previously (31); the mean chi-square value for the best fit was used for analysis of the indicated number of cells.

TRPV4-CFP signal	TRPV1-eYFP	TRPV4-eYFP	TRPA1-eYFP
FRET efficiency	11	18	9
Mean chi-square value	0.039	0.027	0.033
Number of cells tested	32	81	72